UNIVERSITY OF CALIFORNIA, SAN DIEGO

Diffusional Methane Fluxes within Continental Margin Sediments and Depositional Constraints on Formation Factor Estimates

A Thesis submitted in partial satisfaction of the requirements
for the degree Master of Science

in

Earth Sciences

by

Richard D. Berg

Committee in charge:

Professor Miriam Kastner, Chair
Professor Neal Driscoll
Professor David Hilton

2008

The Thesis of Richard D. Berg is approved, and it is acceptable in quality and form for publication on microfilm:

_____

_____

_____

Chair

University of California, San Diego

2008

TABLE OF CONTENTS

Signature Page iii

Table of Contents iv

List of Figures vi

List of Tables vii

Acknowledgements viii

Abstract ix

Chapter 1 Diffusional Methane Fluxes within Continental Margin Sediments
- 1.1 Abstract 1
- 1.2 Introduction 1
- 1.3 Diagenetic Processes in Marine Sediments 2
  - 1.3.1 Marine Sedimentary Organic Matter Oxidation 2
    - 1.3.1.1 General Sequence 2
    - 1.3.1.2 Sulfate Reduction Zone 4
    - 1.3.1.3 Methanogenesis 4
  - 1.3.2 Anaerobic Oxidation of Methane 4
  - 1.3.3 Molecular Diffusion 6
    - 1.3.3.1 Fick's First Law in Porous Media 6
    - 1.3.3.2 Whole-Sediment Diffusion Coefficient 7
- 1.4 Methodology 9
  - 1.4.1 Site Selection 9
  - 1.4.2 Sediment and Interstitial Water Properties 11
    - 1.4.2.1 Measurement of Sulfate Concentrations 11
    - 1.4.2.2 Sulfate Profiles 12
    - 1.4.2.3 Average Porosity 13
    - 1.4.2.4 Tortuosity and Average Formation Factor 14
    - 1.4.2.5 Molecular Diffusion Coefficient 14
    - 1.4.2.6 Average Total Organic Carbon 15
    - 1.4.2.7 Average Grain Density 15
  - 1.4.3 Site Characteristics 15
    - 1.4.3.1 Water Depth 15
    - 1.4.3.2 Sedimentation Rate 15
    - 1.4.3.3 Organic Carbon Accumulation Rate 16
    - 1.4.3.4 Diffusional Sulfate Flux 16

1.5 Sites 17
1.5.1 Location Map for ODP and IODP Sites 17
1.5.2 Tables of Sites 18
1.5.2.1 Subduction Zone Table..... 18
1.5.2.2 Non-Subduction Margin Table..... 19
1.6 Results and Discussion 20
1.6.1 Margin Data 20
1.6.1.1 Consistency of Sulfate Fluxes with Literature 24
1.6.2 Diffusional Methane Fluxes 25
1.6.3 Qualitative "High-Flux" Sites 29
1.7 Conclusions 33
1.8 References 34

Chapter 2 Depositional Constraints on Formation Factor Estimates
2.1 Abstract 38
2.2 Introduction 38
2.3 Methodology 40
2.3.1 Collection of Data 40
2.3.2 Consistency between Depth Intervals 41
2.3.3 Data Quality 42
2.3.4 Calculation of Averages 43
2.3.5 Depositional Environments 44
2.3.6 Lithologies 45
2.3.7 Water Depth 46
2.4 Sites 47
2.5 Results and Discussion 50
2.5.1 Formula Comparison 50
2.5.1.1 Determination of Uncertainty 50
2.5.1.2 Continental Margin Sites 54
2.5.1.3 Basin and Ridge Sites 57
2.5.2 Effect of Depositional Environment 59
2.5.3 Consistency between Depth Intervals 62
2.6 Conclusions 66
2.7 References 67

Appendix A ODP and IODP Drilling Site Descriptions for Chapter 1 68

Appendix B DSDP, ODP, and IODP Data Sources 72

LIST OF FIGURES

Figure 1.1. Marine sedimentary organic matter oxidation sequence ……... 3

Figure 1.2. Map of ODP and IODP sites used for Chapter 1 …… 17

Figure 1.3a. Plot of diffusive sulfate flux versus organic carbon accumulation rate at subduction zone sites and non-subduction zone sites ……. 27

Figure 1.3b. Regression plot (solid lines), with 95% confidence intervals (dashed lines) ……..……... 28

Figure 1.4. Plot showing how diffusive sulfate flux increases exponentially as SMTZ depth decreases ……... 31

Figure 1.5. Plot shows decreasing SMTZ depth with increasing organic carbon accumulation rate …… 33

Figure 2.1. Plot of sulfate-methane transition zone (SMTZ) depth versus linear sulfate concentration gradient ...…….. 42

Figure 2.2. Plot of continental margin data showing Archie formula trend lines . 51

Figure 2.3. Plot of continental margin data showing trend lines of formula used by Iversen and Jorgensen, (1993) …… 51

Figure 2.4. Plot of continental margin data showing Boudreau, (1996), formula trend lines …… 52

Figure 2.5. Plot of deep ocean basin and ridge data showing Archie trend lines .. 52

Figure 2.6. Plot of deep ocean basin and ridge data showing trend lines of formula used by Iversen and Jorgensen, (1993) ……... 53

Figure 2.7. Plot of deep ocean basin and ridge data showing Boudreau, (1996), formula trend lines …….. 53

Figure 2.8. Plot of continental margin data from top 10m of sediment …… 64

Figure 2.9. Plot of continental margin data from top 50m of sediment …… 64

Figure 2.10. Plot of deep ocean basin and ridge data from top 10m of sediment ... 65

Figure 2.11. Plot of deep ocean basin and ridge data from top 50m of sediment ... 65

LIST OF TABLES

Table 1.1. Subduction zone margin sites ……. 18

Table 1.2. Non-subduction margin sites …….. 19

Table 1.3. Data table for subduction zone sites ……... 21

Table 1.4. Data table for non-subduction zone sites …… 22

Table 1.5. Comparison of calculated fluxes with previously published fluxes ... 24

Table 1.6. Qualitative "high-flux" site data ……. 32

Table 2.1. Equations relating formation factor and porosity which utilize a single adjustable constant …….. 39

Table 2.2. ODP site data for 0-10 mbsf depth interval …… 47

Table 2.3. ODP site data for 0-50 mbsf depth interval …… 48

Table 2.4. Analysis of continental margin data …… 56

Table 2.5. Analysis of deep ocean basin and ridge data …….. 58

Table 2.6. Comparison of Archie's formula exponent values from shallow versus deep depth intervals, with uncertainties …….. 60

Table 2.7. Comparison of Archie's formula exponent values from shallow versus deep depth intervals, with uncertainties …….. 60

Table 2.8. Exponent with uncertainty for Archie's formula based on sediment lithology and depositional environment with porosity less than 0.70 . 66

Table 2.9. Exponent with uncertainty for Archie's formula based on sediment lithology and depositional environment with porosity greater than 0.70 …….. 66

ACKNOWLEDGEMENTS

I would like to thank Professor Miriam Kastner for all the advice and opportunities given to me, from picking up leaves to running an ion chromatograph.

I'd also like to thank Gretchen Robertson, Evan Solomon, and Wei Wei for their help in the lab and answering random questions.

I'm grateful to Caren Duncanson, Pamela Buaas, and Jane Teranes for helping me navigate the Earth Sciences program.

For their advice and direction on the progress of my research, I'd like to thank Professor Dave Hilton and Professor Neal Driscoll of my thesis committee.

Thank you Bruce Deck for help figuring out the instruments in the analytical lab, and the random news stories.

Lastly, I'd like to thank my family, Mom, Dad and Victoria, Marea and Justin, Brent and Chasity, and Blythe, for their support during my entire college career and life.

ABSTRACT OF THE THESIS

Diffusional Methane Fluxes within Continental Margin Sediments and Depositional Constraints on Formation Factor Estimates

by

Richard D. Berg

Master of Science in Earth Sciences

University of California, San Diego, 2008

Professor Miriam Kastner, Chair

Diffusion and reaction of chemical species in ocean sediments are important processes in global cycles of carbon, sulfur, and other elements. Chapter 1 explores the processes in continental margin sediments that supply a diffusional flux of methane to the upper sediment column, where methane is consumed in a net reaction with sulfate. Data obtained from the Ocean Drilling Program (ODP), and Integrated

Ocean Drilling Program (IODP) show that, in general, in subduction zone sediments, more methane is being consumed for the amount of methane being microbially produced *in situ* than in divergent margin and non-subduction convergent margin (such as the California margin south of Mendocino) sediments.

Chapter 2 provides a new way to decrease the uncertainty involved in estimating sediment tortuosity using porosity, lithology, and depositional environment. By compiling ODP formation factor and porosity data from sites with differing lithologies and depositional environments, it is shown that depositional environment may provide an additional constraint when estimating the relationship between porosity and formation factor using Archie's formula (Archie, 1942). Reducing the uncertainty of formation factor estimates can reduce the uncertainty of tortuosity and molecular diffusional flux calculations for natural sediments.

CHAPTER 1

Diffusional Methane Fluxes within Continental Margin Sediments

1.1 Abstract

Sulfate fluxes, used as a proxy for methane fluxes, were compared with organic carbon accumulation rates at margin sites of the Ocean Drilling Program (ODP) and Integrated Ocean Drilling Program (IODP) in order to determine differences in methane consumption and production rates in the sediments along the continental margins. The sediments of subduction zone margins were found to have greater diffusional methane fluxes to the sulfate-methane transition zone than non-subduction convergent margins and divergent margins with similar *in situ* methane production rates, implying subduction zones have additional methane being supplied to the upper sediments. Greater advection of methane-rich fluid in subduction zone sediments not only affects advective fluxes of methane into the overlying ocean (e.g., Schlüter, 2002), but may also increase the diffusive fluxes of methane and, in turn, sulfate, to the sulfate-methane transition zone.

1.2 Introduction

Microbially-mediated methane oxidation in anoxic marine sediments is an important process for methane consumption in the global carbon cycle. It serves as a barrier to the methane generated in marine sediments from reaching the overlying seawater, where it could have a significant effect on ocean chemistry and benthic organisms. The methane is oxidized by a consortium of microbes, with sulfate acting as the terminal electron acceptor (Hoehler et al., 1994, Boetius et al., 2000). The

reduction of sulfate in marine sediments associated with methane oxidation is also a significant sink for sulfate in the ocean.

Continental margin sediments are particularly important marine environments for the anaerobic oxidation of methane. Methane consumption has been shown to be orders of magnitude greater in continental margin sediments than deep ocean basin sediments (D'Hondt et al., 2002). Here, I compare rates of diffusional methane oxidation, using diffusional sulfate flux as a proxy, along different types of continental margins. Diffusional fluxes of sulfate at subduction zone margins are compared with those at non-subduction convergent margins and divergent margins in order to explore the processes controlling the magnitudes of diffusional fluxes of methane being oxidized in different types of continental margins.

Porewater and sedimentation data from continental margin sites of the Deep Sea Drilling Project (DSDP), the Ocean Drilling Program (ODP), and the Integrated Ocean Drilling Program (IODP) were compiled and analyzed. The rates of sulfate reduction involved in the oxidation of methane were compared with rates of organic carbon accumulation to determine the relationships between methane production and consumption in continental margin sediments.

1.3 Diagenetic Processes in Marine Sediments

1.3.1 Marine Sedimentary Organic Matter Oxidation

1.3.1.1 General Sequence

Oxidants are reduced by organic matter down the sediment column in a succession of microbially mediated reactions (Claypool and Kaplan, 1974, Froelich et

al., 1979). This ecological succession is thought to be primarily structured by the energy yield of each reaction, with the highest energy-yielding reactions occurring in the top centimeters of the sediment column, the next highest energy-yielding reaction dominating once the first oxidant is depleted, and so on.

The first oxidant to be utilized by bacteria is molecular oxygen, followed by nitrate once the oxygen is depleted. Manganese and iron oxy-hydroxides are the next to be utilized, though the exact place in the sequence of these two minor oxidants is not always consistent (Froelich et al., 1979). Along continental margins, all four of these oxidants are commonly depleted within centimeters of the sediment surface. Sulfate is the next oxidant that gets depleted. Once sulfate is depleted, methane concentrations increase due to the activity of methane-generating archaea (Claypool and Kaplan, 1974).

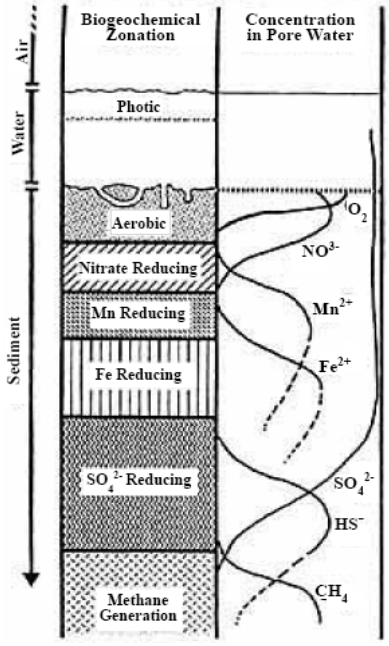

Figure 1.1. Marine sedimentary organic matter oxidation sequence. Figure modified from Eganhouse and Venkatesan (1993).

1.3.1.2 Sulfate Reduction Zone

The depth interval in the sediment column in which sulfate is depleted by the activity of sulfate-reducing bacteria is known as the sulfate reduction zone. In this zone, organic molecules are oxidized by sulfate in the microbially-mediated net reaction (e.g., Berner, 1980):

$$2CH_2O + SO_4^{2-} \rightarrow H_2S + 2HCO_3^- \quad (1.1)$$

The sulfate reduction zone commonly occupies a much greater depth interval than the reduction zones of oxygen, nitrate, manganese oxide, or iron oxide due to sulfate's much greater concentration in the ocean (Froelich et al., 1979).

1.3.1.3 Methanogenesis

Below the sulfate reduction zone, methane concentrations increase to significant levels due to archaea which produce methane as a metabolic byproduct (Claypool and Kaplan, 1974). The two principal pathways for methanogenesis are fermentation of acetate (Eqn. 1.2) and reduction of CO_2 by H_2 (Eqn. 1.3) (e.g., Reeburgh, 2007).

$$CH_3COOH \rightarrow CO_2 + CH_4 \quad (1.2)$$

$$4H_2 + CO_2 \rightarrow CH_4 + 2H_2O \quad (1.3)$$

Reaction 1.3 is more common in marine sediments since sulfate-reducing bacteria deplete the available acetate (Whiticar, 1999).

1.3.2 Anaerobic Oxidation of Methane

Between the sulfate reduction zone, where sulfate is depleted, and the methanogenesis zone, where methane concentrations reach significant levels, is a

centimeter-scale depth interval that is known as the sulfate-methane transition zone (SMTZ). At the SMTZ, a consortium of archaea and bacteria consume sulfate and methane in a process known as anaerobic oxidation of methane (AOM); (Hoehler et al., 1994, Boetius et al., 2000). The bacteria consume the sulfate, while the archaea consume the methane in what may be a reverse process of methanogenesis (Hoehler et al., 1994, Hansen et al., 1998, Hinrichs et al., 1999). Although the exact reaction pathway is not known, the resulting net reaction (Eqn. 1.4) has been found to consume sulfate and methane in a one-to-one net reaction (Barnes and Goldberg, 1976, Reeburgh, 1976).

$$SO_4^{2-} + CH_4 \rightarrow HS^- + HCO_3^- + H_2O \qquad (1.4)$$

AOM produces a linear sulfate concentration gradient characteristic of diffusion of sulfate to a reactive layer, from an overlying source of constant concentration (Borowski, 1996). This linear concentration profile is distinct from the concave-down sulfate concentration profile created by the reduction of sulfate by organic matter within the sulfate reduction zone (e.g., Berner, 1980).

A significant difference between the two processes by which sulfate is reduced in marine sediments is that AOM produces one mole of carbon dioxide for every mole of sulfate reduced (see Eqn. 1.4), while sulfate reduction by organic matter produces two moles of carbon dioxide for every mole of sulfate (see Eqn. 1.1). This difference may be seen in the depth-concentration profiles of sulfate and alkalinity. In areas where sulfate reduction is dominated by AOM, sulfate and alkalinity should both have linear concentration profiles with nearly equal slopes, but opposite sign (Borowski,

1996). In areas where AOM is insignificant, and oxidation of organic matter in the sulfate-reduction zone is the dominant sulfate reduction pathway, the slope of alkalinity should be curved concave-down, and have about twice the magnitude of the sulfate slope, with opposite sign (e.g., Berner, 1980, Gieskes, 1981).

1.3.3 Molecular Diffusion

1.3.3.1 Fick's First Law in Porous Media

Diffusion of molecules in a solution is mathematically described by Fick's first law of diffusion:

$$J = -D\frac{\partial C}{\partial x} \tag{1.5}$$

where J is diffusive flux, D is the diffusion coefficient, and $\frac{\partial C}{\partial x}$ is the concentration gradient in the x direction.

In saturated porous media, namely marine sediments, the formula becomes (Berner, 1980):

$$J = -\varphi D_s \frac{\partial C}{\partial x} \tag{1.6}$$

where φ is porosity and D_s is the whole-sediment diffusion coefficient.

1.3.3.2 Whole-Sediment Diffusion Coefficient

The whole-sediment diffusion coefficient is described by the formula (Berner, 1980):

$$D_s = \frac{D_{pw}}{\theta^2} \tag{1.7}$$

where D_{pw} is the diffusion coefficient in porewater, and θ is the tortuosity of the sediment.

The tortuosity is the path length a molecule must take through sediment, divided by the straight-line distance. The square of the tortuosity has been empirically shown to be equal to the porosity multiplied by the formation factor (Mcduff and Ellis, 1979, Ullman and Aller, 1982):

$$\theta^2 = \varphi F \tag{1.8}$$

where F is the formation factor. This relationship between tortuosity, porosity, and formation factor has also been shown to have a theoretical basis using an inclined capillary model (Cornell and Katz, 1953, Bear, 1972, Ullman and Aller, 1982). Using this relationship, the formula for the whole-sediment diffusion coefficient becomes:

$$D_s = \frac{D_{pw}}{\varphi F} \tag{1.9}$$

The formation factor is defined as the ratio of the resistivity of the bulk saturated sediment (ρ_s) to the resistivity of the interstitial fluid (ρ_i) (Archie, 1942). As such, the formation factor is inversely proportional to the porosity. The formation factor has a natural lower limit of 1 when the pore volume ratio reaches a (theoretical) value of 1 since both resistivities would be those of only the fluid. Here, it is assumed

that all pores are interconnected, that the sediment is not significantly conductive compared to the interstitial water, and that the effect of the surface charges on sediment grains does not have a significant effect on the resistivity measurement. These three assumptions are reasonable at the porosities encountered in this study.

An empirical formula was proposed by Archie, (1942) that relates formation factor to porosity:

$$F = \varphi^{-n} \tag{1.10}$$

where n is an adjustable constant. The equation describes the exponential increase in formation factor with linearly decreasing porosity. Archie proposed an exponent of 1.8-2 for consolidated sandstones and an exponent of, "about 1.3 for clean, unconsolidated sands." (Archie, 1942). Using Archie's formula, the equation for the whole-sediment diffusion coefficient becomes:

$$D_s = \frac{D_{pw}}{\varphi^{-n+1}} \tag{1.11}$$

and Fick's first law in porous media becomes:

$$J = \frac{\varphi D_{pw}}{\varphi^{-n+1}} \frac{\partial C}{\partial x} = \varphi^n D_{pw} \frac{\partial C}{\partial x} \tag{1.12}$$

As it will be shown in Chapter 2, Archie's formula provides a reliable estimate for formation factor only if good constraints are available for the exponent, on the basis of lithology and depositional environment.

1.4 Methodology

1.4.1 Site Selection

Potential sites were constrained by their geological setting, data availability and quality, and lithology. Sites from DSDP (sites 1-624), ODP (sites 626-1277), and IODP (sites 1301-1329) were considered. Sites were required to be located on a continental slope and have high-quality porewater sulfate concentration data. A slope environment is considered to be on a continental margin, below the continental shelf, and is defined by gradient. However, for this study, the continental slope category includes the entire margin that is at a water depth of 200 meters or more, which may include continental shelf below 200 meters water depth in addition to continental slope. The slope category is above the topographically distinct continental rise and basin environment, which are distinguished in cross-section.

In order to identify possible sites for use, possible continental slope sites were selected using the DSDP/ODP/IODP world map of drill sites (Figure 1.2) published by the IODP. Sites clearly located outside of a continental margin were eliminated from consideration. Also, sites located within evaporative basins (e.g. Gulf of Mexico, Mediterranean Sea) were not considered due to the possibility of diffusion of sulfate from underlying salt brines. The individual site maps of the drilling legs of the remaining sites were then examined to determine which sites were located on the continental slope. For drilling expeditions with inadequately detailed published site maps, the site reports had to be examined in order to determine the geologic settings of

the sites. The site reports often contain both site descriptions and seismic profiles, which illustrate the geologic settings.

After geographically constraining the sites, porewater sulfate concentration data were gathered from the Initial Reports of the DSDP and ODP. Also, sulfate concentrations of sites 1326, 1327, and 1329 from IODP Expedition 311, which were the only IODP sites that qualified for use, were independently measured using inductively-coupled plasma mass spectrometry. Other sites with no published sulfate data are omitted. Since at least three measurements are required to obtain a regression line with an uncertainty less than 100%, sites with less than three measurements before sulfate concentrations reach background levels are also omitted, with the exception of those reaching background levels at 10 mbsf or less, which are classified as high-flux sites with unknown magnitudes (see section 1.6.3.1). Sites with sulfate concentrations that increase with depth are omitted due to their association with sub-seafloor brines or some other sub-seafloor source of concentrated sulfate. The data must be consistent with a steady-state diffusional profile, that is, either discernibly concave-down, or linear with a regression fit with less than 40% uncertainty with a 95% confidence interval. Sulfate data with excessive scatter could not be used with a reasonable amount of statistical certainty. Due to this requirement, all DSDP sites are omitted from this study.

After identifying continental slope sites with linear sulfate concentration profiles, the lithologies were examined to ensure that the linearity was more likely due to anaerobic oxidation of methane (AOM) rather than an result of the organic matter

distribution in the sediment column. For example, at sites from ODP Leg 159 at the Demerara Rise, the profile of total organic carbon (TOC) shows very low TOC from the seafloor to a subseafloor depth of 400 meters, where there is a sharp increase in TOC, and the sulfate concentration profile shows a linear gradient that reaches background concentrations at 400 mbsf. It is likely that the linear profile is caused by relatively high rates of organic matter oxidation within the high-TOC layer rather than anaerobic oxidation of methane. Those sites with linear sulfate concentration profiles that are likely shaped by organic matter distribution, such as the sites of ODP Leg 159, are omitted.

As an additional measure for the dominance of AOM in the system, the alkalinity-depth profiles were compared with the sulfate concentration-depth profiles. Alkalinity profiles should be nearly the inverse of the sulfate concentration profiles in an AOM dominated system, and double the inverse in a system dominated by sulfate reduction of non-methane organic molecules in the sulfate reduction zone. Those sites with alkalinity profiles that were representative of the latter were omitted.

1.4.2 Sediment and Interstitial Water Properties

1.4.2.1 Measurement of Sulfate Concentrations

Interstitial water samples extracted from sediment cores obtained during IODP expedition 311 were measured for sulfate concentration using inductively-coupled plasma optical emission spectrometry (ICP-OES). Sulfate concentration profiles were measured for sites 1325, 1326, 1327, 1328, and 1329, with depth intervals of less than one meter between samples. Sulfate concentrations at sites 1325 and 1328 decreased

to background levels at such shallow depths, not enough data points were available to calculate a concentration gradient.

The samples had already been collected and treated with a cadmium nitrate solution in order to precipitate reduced sulfur species, leaving behind sulfate as the only sulfur species in solution. Samples were then diluted to 1/200th concentration using a 1% HNO_3 solution and the sulfur concentrations were measured.

A calibration curve was made using five calibration standards. The standards were IAPSO seawater diluted with 1% HNO_3 solution to 1/150th, 1/200th, 1/300th, 1/600th, and 1/5000th seawater concentrations. The correlation coefficient for the calibration curve for sulfur was 0.999976.

A solution of dilute IAPSO seawater with known concentration was ran after every tenth sample. The sulfate concentrations of these prepared samples were measured with a relative standard deviation of 1.1% from the average concentration, showing high relative precision. Also, every tenth sample, beginning with the fifth sample, was run in duplicate in order to test for absolute precision. The greatest measured concentration difference between two duplicates was 0.2 mM.

1.4.2.2 Sulfate Profiles

The values of the linear sulfate concentration gradients of the porewater are determined using a linear least squares regression of the sulfate concentrations versus depth below seafloor. The sulfate-methane transition zone (SMTZ) or the depth at which sulfate concentration becomes zero, is determined by the intercept of the regression line with the “depth below seafloor” axis.

The 2σ deviation of the regression is calculated using the formula:

$$2\sigma = 2 \times \frac{dC}{dz} \times \sqrt{\frac{\frac{1}{r^2} - 1}{P - 2}} \tag{1.13}$$

where σ is the standard deviation, dC/dz is the linear sulfate concentration gradient, r^2 is the correlation coefficient, and P is the number of data points used for the regression fit.

Many profiles exhibit constant seawater concentrations of sulfate in the porewater of the top few meters of sediment, followed by a linear decrease in concentration to background levels. These concentration profiles may occur due to bioirrigation or rapid sedimentation events such as debris flows (Hensen et al., 2003). In these cases, the initial constant concentrations are not used in the regression. Rather, the gradient is calculated using the points of decreasing concentration.

1.4.2.3 Average Porosity

ODP and IODP porosity data were gathered from the IODP online database for each selected site. The porosity data used are from below the seafloor to the datum nearest the SMTZ. The methods used to calculate average porosity for each site are described in Section 2.3.4. An uncertainty of 10% is estimated for average porosity values.

1.4.2.4 Tortuosity and Average Formation Factor

Tortuosity is calculated as described in Section 1.3.3.2 using this formula (derived from Equation 1.8):

$$\theta = \sqrt{\varphi F} \tag{1.14}$$

where θ is tortuosity, φ is porosity, and F is formation factor. Formation factors for sites without measured formation factor data are estimated using Archie's formula with an exponent value based on depositional environment and lithology. Each site is categorized by its depositional environment and lithology; then an Archie's formula exponent value is assigned to the site using the results of Chapter 2. The uncertainties of formation factor values are calculated using the uncertainties in porosity and Archie exponent values using the formula:

$$\varepsilon_F = \sqrt{(-n\varphi^{-(n+1)})^2 \varepsilon_\varphi^{\,2} + (-\varphi^{-n}\ln(\varphi))^2 \varepsilon_n^{\,2}} \tag{1.15}$$

where ε is the uncertainty, φ is porosity, and n is the Archie exponent.

For sites with formation factor data, the data are from the Initial Reports of the ODP for each site. No formation factor data are available for the IODP sites. The formation factor data used are from below the seafloor to the datum nearest the SMTZ. The methods used to calculate average formation factor are described in Section 2.3.4. An uncertainty of 10% is estimated for all average formation factor values obtained from measured formation factors.

1.4.2.5 Molecular Diffusion Coefficient

The molecular diffusion coefficient of sulfate in seawater at a temperature of 5 +/- 0.3°C has been experimentally shown to be 5.8 x 10^{-6} cm^2/sec (Li and Gregory,

1974). This value is used with an estimated uncertainty of 10% for all sites. This uncertainty value is reasonable for a sub-seafloor temperature gradient of 0.1°C/m and interstitial water salinity similar to seawater. The effect of pressure on the molecular diffusion coefficient is insignificant (Horne et al., 1969, Li and Gregory, 1974).

1.4.2.6 Average Total Organic Carbon

Total organic carbon data for both ODP and IODP sites are from the IODP online database. Average values are estimated for the depth interval of about the depth to the SMTZ, below the SMTZ.

1.4.2.7 Average Grain Density

Grain density data for both ODP and IODP sites are from the IODP online database. Average values are estimated for a depth interval of about the depth to the SMTZ, below the SMTZ

1.4.3 Site Characteristics

1.4.3.1 Water Depth

Site water depths are depths of the seafloor from sea level, and were obtained from the IODP online database and can be found in the Initial Reports of the ODP and IODP.

1.4.3.2 Sedimentation Rate

Sedimentation rates are for the upper sediment column, and obtained from the Initial Reports of the ODP and IODP.

1.4.3.3 Organic Carbon Accumulation Rate

A rough average organic carbon accumulation rate (OCAR) for each site was calculated using the formula:

$$OCAR = S \times (1 - \varphi) \times D \times \left(\frac{C}{100} \right) \tag{1.16}$$

where S is the sedimentation rate, φ is average porosity, D is average grain density, and C is average total organic carbon in weight percent.

1.4.3.4 Diffusional Sulfate Flux

Diffusional sulfate flux into the sediment from the overlying seawater is calculated using Fick's first law of diffusion, applied to a porous medium, using equations 1.6 and 1.12.

1.5 Sites

Sulfate fluxes significantly driven by AOM are calculated for a total of 42 sites from 12 ODP legs and 1 IODP expedition. Site location descriptions are included in Appendix A.

1.5.1 Location Map for ODP and IODP Sites

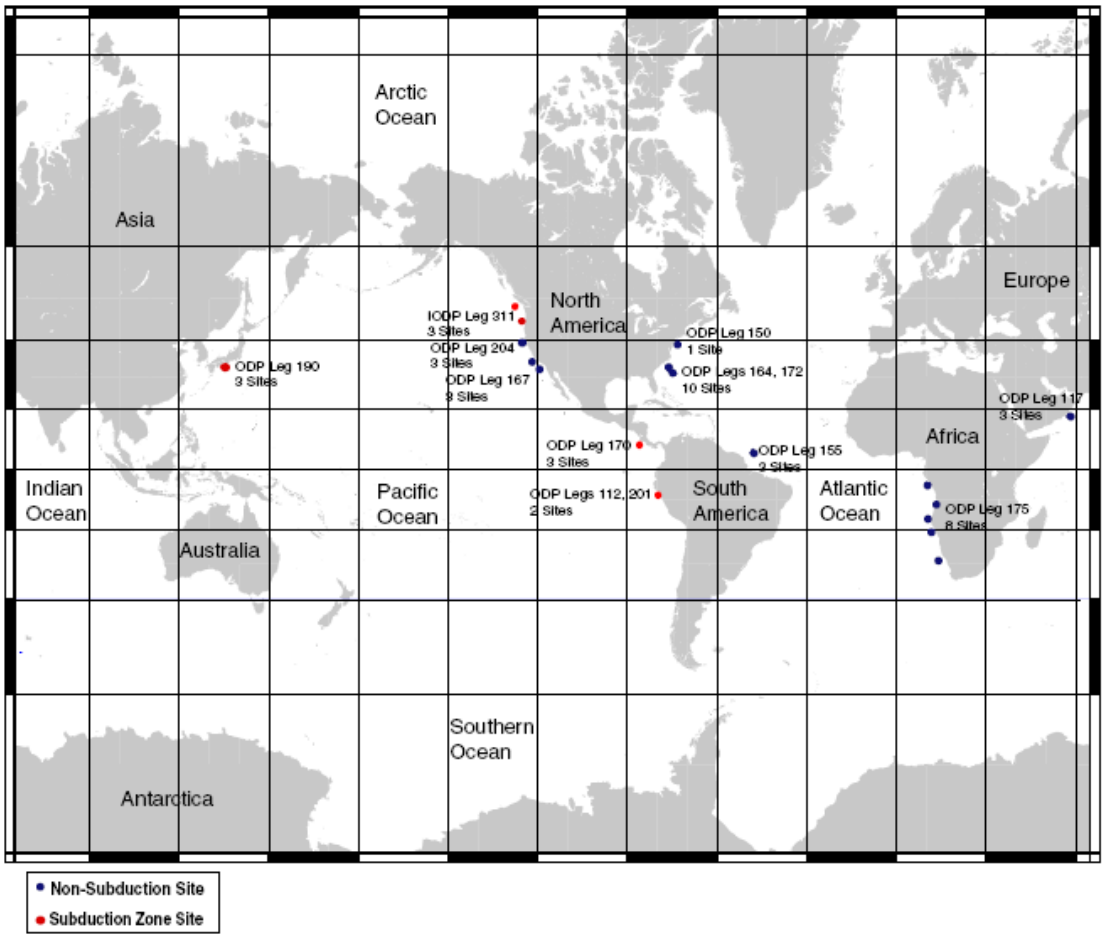

Figure 1.2. Map of ODP and IODP sites used for Chapter 1.

1.5.2 Tables of Sites

1.5.2.1 Subduction Zone Table

Table 1.1. Subduction zone sites.

Margin	Leg	Site	Water Depth (mbsl)
Peru	112	684	438
Middle America	170	1040	4177
		1041	3306
		1043	4313
Nankai	190	1175	2998
		1176	3021
		1178	1742
Peru	201	1227	427
Cascadia	204	1244	895
		1245	869
		1247	834
Cascadia	311	1326	1828
		1327	1305
		1329	950

1.5.2.2 Non-Subduction Margin Table

Table 1.2. Non-subduction margin sites.

Margin	Leg	Site	Water Depth (mbsl)
Oman	117	723	805
		724	591
		728	1422
Eastern North America	150	906	913
Amazon	155	931	3475
		940	3191
		944	3701
Blake Ridge	164	991	2568
		993	2642
		994	2798
		995	2777
		997	2770
California	167	1013	1564
		1017	955
		1022	1926
Blake Ridge	172	1054	1294
		1055	1798
		1059	2985
		1060	3481
		1061	4044
Western Africa	175	1075	2995
		1076	1404
		1077	2380
		1078	427
		1079	738
		1082	1279
		1083	2178
		1085	1713

1.6 Results and Discussion

1.6.1 Margin Data

The ODP and IODP continental margin sites are categorized as being located in either a subduction zone or non-subduction margin. The non-subduction margin sites are all located on divergent margins with the exception of sites 1013, 1017, and 1022 from ODP Leg 167, which are located on the California margin south of the Mendocino Triple Junction.

The diffusive sulfate flux of each site was calculated from measured data, with estimated uncertainties between 14% and 34% for subduction zone sites and between 14% and 37% for non-subduction margin sites (Tables 1.3 and 1.4).

Table 1.3. Data table for subduction zone sites. sili.= siliceous ooze. calc.= calcareous ooze. I.D.= insufficient data. See Methods section for data sources. See section 1.3.3.2 for definition of Formation Factor.

Location	Leg	Site	Major Lithology	Minor Lithology	SMTZ Depth (mbsf)	Sulfate Concentration Gradient (mmol m^{-1})	Formation Factor	Average Porosity	Diffusive Sulfate Flux (mol m^{-2} y^{-1})	Error (%)	Organic Carbon Accumulation Rate (g m^{-2} y^{-1})
Cascadia											
	204	1244	mud		8.3	5.37	3.09	0.64	3.18E-02	28	3.2
		1245	mud	sand	6.8	7.33	2.84	0.63	4.73E-02	29	2.1
		1247	mud		10.7	5.50	3.19	0.63	3.16E-02	28	1.3
	311	1326	mud		2.5	12.20	4.56	0.55	4.90E-02	34	1.1
		1327	mud		7.9	4.21	3.62	0.60	2.13E-02	30	1.2
		1329	mud		9.0	4.00	3.10	0.64	2.36E-02	28	0.6
Peru											
	112	684	mud	sili.	22.6	0.92	2.45	0.74	6.89E-03	29	0.7
	201	1227	mud	sili.	45.4	0.16	2.53	0.72	1.15E-03	15	0.5
Middle America											
	170	1040	mud	sand	19.8	1.34	3.26	0.56	7.52E-03	18	0.8
		1041	mud		16.0	1.52	3.46	0.61	8.05E-03	31	0.9
		1043	mud	breccia	18.6	1.75	2.61	0.69	1.23E-02	20	0.5
Nankai											
	190	1175	mud	calc.	14.0	1.00	3.14	0.64	5.83E-03	15	I.D.
		1176	mud	calc.	18.2	1.03	2.68	0.68	7.03E-03	14	0.9
		1178	mud	calc.	32.2	0.93	3.48	0.60	4.87E-03	16	0.2

Table 1.4. Data table for non-subduction margin sites. sili.= siliceous ooze. calc.= calcareous ooze. I.D.= insufficient data. See Methods section for data sources. See section 1.3 for definition of SMTZ and Formation Factor.

Location	Leg	Site	Major Lithology	Minor Lithology	SMTZ Depth (mbsf)	Sulfate Concentration Gradient (mmol m^{-1})	Formation Factor	Average Porosity	Diffusive Sulfate Flux (mol m^{-2} y^{-1})	Error (%)	Organic Carbon Accumulation Rate (g m^{-2} y^{-1})
California											
	167	1013	mud	calc.	19.0	1.59	3.14	0.72	9.26E-03	32	0.5
		1017	mud		13.3	3.21	3.40	0.61	1.73E-02	30	1.7
		1022	mud	calc.	31.0	0.82	3.52	0.63	4.27E-03	29	I.D.
Eastern North America											
	150	906	mud		28.9	0.87	4.84	0.53	3.27E-03	36	0.7
	164	991	mud	calc.	42.0	0.65	3.11	0.66	3.81E-03	27	1.6
		993	mud	calc.	24.5	2.17	5.25	0.55	7.56E-03	36	3.4
		994	mud	calc.	21.5	1.18	2.98	0.67	8.71E-03	27	0.1
		995	mud	calc.	21.7	1.25	2.75	0.69	8.31E-03	25	0.2
		997	mud	calc.	22.5	1.23	2.89	0.68	7.80E-03	26	0.3
	172	1054	mud	calc.	50.3	0.66	3.57	0.70	3.37E-03	27	0.2
		1055	mud	calc.	26.9	1.03	2.84	0.66	6.63E-03	14	0.9
		1059	mud	calc.	9.3	3.12	2.85	0.72	2.00E-02	17	0.4
		1060	mud	calc.	12.3	2.34	2.50	0.76	1.71E-02	14	0.9
		1061	mud	calc.	16.8	1.59	2.77	0.74	1.05E-02	14	1.1
Eastern South America											
	155	931	mud	calc.	6.2	4.61	3.43	0.70	2.46E-02	28	18.7
		940	mud		37.2	0.56	3.19	0.63	3.22E-03	30	107.6
		944	mud	calc.	3.7	6.44	2.92	0.74	4.03E-02	26	I.D.
Oman											
	117	723	mud	calc.	46.5	0.51	3.33	0.65	2.81E-03	33	1.4
		724	mud	calc.	50.2	0.59	4.90	0.56	2.18E-03	37	0.9
		728	mud	calc.	82.4	0.43	4.47	0.58	1.76E-03	32	0.7

Table 1.4 (cont.). Data table for non-subduction margin sites. sili.= siliceous ooze. calc.= calcareous ooze. I.D.= insufficient data. See Methods section for data sources. See section 1.3 for definition of SMTZ and Formation Factor.

Location	Leg	Site	Major Lithology	Minor Lithology	SMTZ Depth (mbsf)	Sulfate Concentration Gradient (mmol m^{-1})	Formation Factor	Average Porosity	Diffusive Sulfate Flux (mol m^{-2} y^{-1})	Error (%)	Organic Carbon Accumulation Rate (g m^{-2} y^{-1})
Western Africa											
	175	1075	mud	sili.	29.7	1.26	1.55	0.87	1.49E-02	20	2.0
		1076	mud	sili.	18.3	1.44	1.77	0.83	1.49E-02	27	3.5
		1077	mud	sili.	21.1	1.60	1.62	0.85	1.81E-02	20	2.0
		1078	mud	calc.	12.8	2.40	3.52	0.63	1.25E-02	32	11.5
		1079	mud	calc.	52.9	0.62	3.67	0.62	3.09E-03	30	11.8
		1082	mud	calc.	21.3	1.75	2.66	0.76	1.20E-02	25	1.7
		1083	calc.		26.7	1.17	2.76	0.75	7.75E-03	26	2.0
		1085	calc.		38.5	0.77	2.79	0.66	5.06E-03	27	1.1

1.6.1.1 Consistency of Sulfate Fluxes with Literature

The calculated diffusive sulfate flux values are consistent with previously published flux values from ODP legs 164, 190, and 201, indicating that the calculated fluxes are reliable within the estimated uncertainties (Table 1.5). However, the published fluxes from ODP Leg 204 in Claypool et al. (2006) are consistently lower than the calculated results, and are even beyond the estimated uncertainty for sites 1244, 1245, 1247, and 1251. The dominant reason for this is that Claypool et al. (2006) use one constant whole-sediment diffusion coefficient of 6000 m^2 ma^{-1} [$1.9x10^{-6}$ cm^2s^{-1}] for all sites, while the calculated whole-sediment diffusion coefficients of the individual sites are greater, in the range of 8200-10200 m^2 ma^{-1} [$2.4\text{-}3.2x10^{-6}$ cm^2s^{-1}]. The lower whole-sediment diffusion coefficient used by Claypool et al. results in proportionally lower fluxes when Fick's first law of diffusion for porous media is used to calculate diffusive sulfate flux.

Table 1.5. Comparison of calculated fluxes with previously published fluxes. Blue indicates literature flux within estimated uncertainty of calculated flux. Orange indicates literature flux outside of estimated uncertainty. 1. Borowski et al., (2000). 2. D'Hondt et al., (2002). 3. D'Hondt et al., (2004). 4. Claypool et al., (2006).

Leg	Site	Literature SO_4 Flux (mol m^{-2} y^{-1})	Calculated SO_4 Flux (mol m^{-2} y^{-1})	Calculated Uncertainty (%)	Percent Difference (%)
164[1]	994	8.8E-03	8.7E-03	27	-1
	995	8.2E-03	8.3E-03	25	1
190[2]	1175	5.6E-03	5.8E-03	15	4
201[3]	1230	2.5E-02	2.7E-02	22	7
204[4]	1244	2.1E-02	3.2E-02	28	34
	1245	2.5E-02	4.7E-02	29	47
	1247	2.0E-02	3.2E-02	28	38
	1251	3.4E-02	5.6E-02	26	38
	1252	3.4E-02	4.6E-02	27	25

1.6.2 Diffusional Methane Fluxes

In order to determine the diffusional flux of methane to the SMTZ, diffusional sulfate flux to the SMTZ is used as a proxy. The linear sulfate concentration gradients, combined with the alkalinity profiles which nearly mirror the sulfate profiles of the sites, suggests that anaerobic oxidation of methane (AOM) dominantly drives the diffusional flux of sulfate at the ODP and IODP sites listed (Borowski, 1996). Since the subsurface AOM rate, which is driving the diffusional sulfate flux, is equal to the flux of methane to the sulfate-methane transition zone (SMTZ) in steady-state, it follows that the calculated diffusional flux of sulfate to the SMTZ is equal to the flux of methane to the SMTZ.

In a diffusional regime, the flux of methane to the SMTZ is supplied by *in situ* methane generation by the microbial degradation of organic matter below the SMTZ (Claypool and Kaplan, 1974). The rate of *in situ* organic matter degradation below the SMTZ is a function of organic matter accumulation rate and the reactivity of the organic matter (e.g., Hedges and Keil, 1995). In most marine sediments, accumulation rate is generally the dominant factor influencing differences in the amount of organic matter degradation, because reactivities are generally similar, and thus less of an influence (Martens, et al., 1998).The influence that the reactivity of organic matter between different sites has on the results should be further minimized by the variety of margins sampled. With the exception of the Amazon Fan, subduction zone and non-subduction margin sites should have a comparable variety of organic matter reactivity. So, at first-order, the accumulation rate of organic matter is proportional to the amount

of methane being produced in the sediments below the SMTZ, and thus the flux of sulfate being consumed during AOM.

Figure 1.3b shows that subduction zone sediments will generally have a greater diffusive sulfate reduction rate driven by AOM than non-subduction margin sediments, for any given organic matter accumulation rate. The 95% confidence intervals of the regression fits shown in figure 1.3b are shown not to overlap, which indicates that the difference in slope of the two regression lines is significant. Similar organic matter accumulation rates, but greater diffusive sulfate reduction rates, indicate that additional methane is diffusing up through the sediment column to the SMTZ than would be expected to be supplied from *in situ* methane production alone. This requires that methane concentrations be increased at some point below the SMTZ, increasing the methane concentration gradient, and thus the upward diffusional methane flux.

Figure 1.3a shows the entire range of organic carbon accumulation rates at the sites. The four non-subduction margin sites with very high accumulation rates of >10 g m^{-2} y^{-1} may have unusually low diffusive sulfate fluxes due to greater preservation of the organic matter. With very high accumulation rates, a greater percentage of the sedimentary organic matter is preserved in the sediment column (e.g., Hedges and Keil, 1995), and thus drives a lesser diffusive sulfate flux than would be expected if the organic matter had time to be oxidized. Figure 1.3a demonstrates this most dramatically with site 940, a site on the Amazon Fan with an organic carbon accumulation rate of 107.6 g m^{-2} y^{-1}. Also, at the Amazon Fan sites, the

reactivity of the organic matter is likely much less than the average, since it is mostly of terrestrial origin (Schlunz et al., 1999), and this is likely to contribute to its preservation in the sediment column.

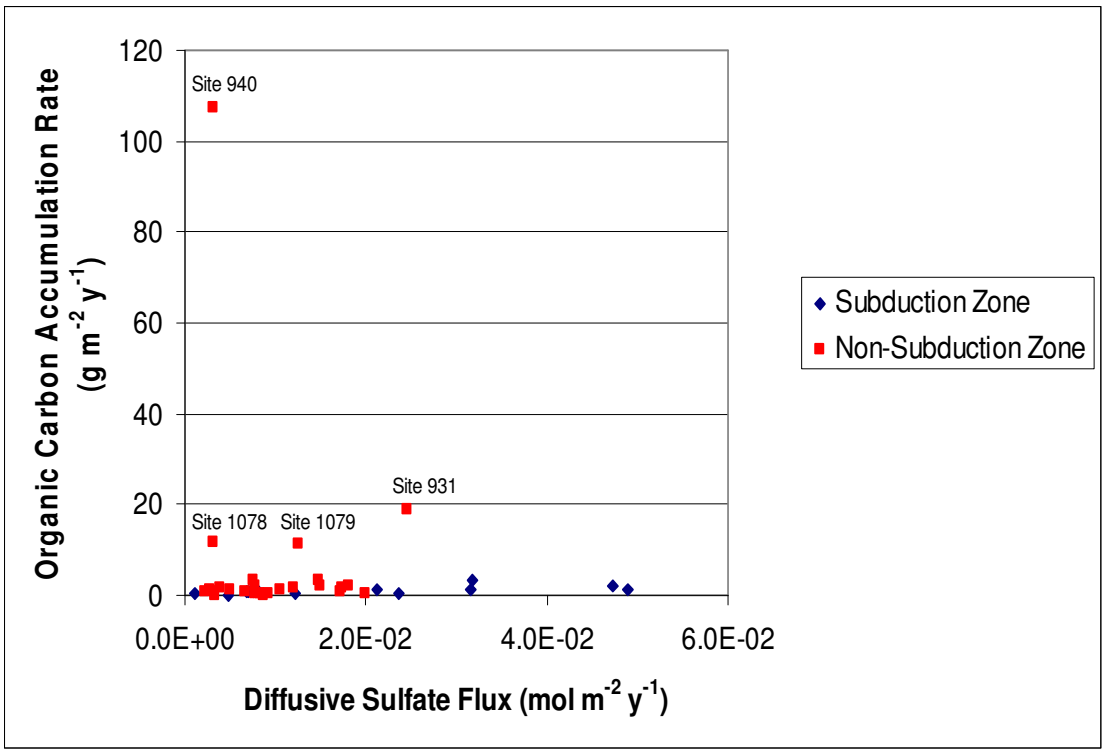

Figure 1.3a. Plot of diffusive sulfate flux versus organic carbon accumulation rate at subduction zone sites and non-subduction margin sites. See table 1.3 and 1.4 for site locations and data.

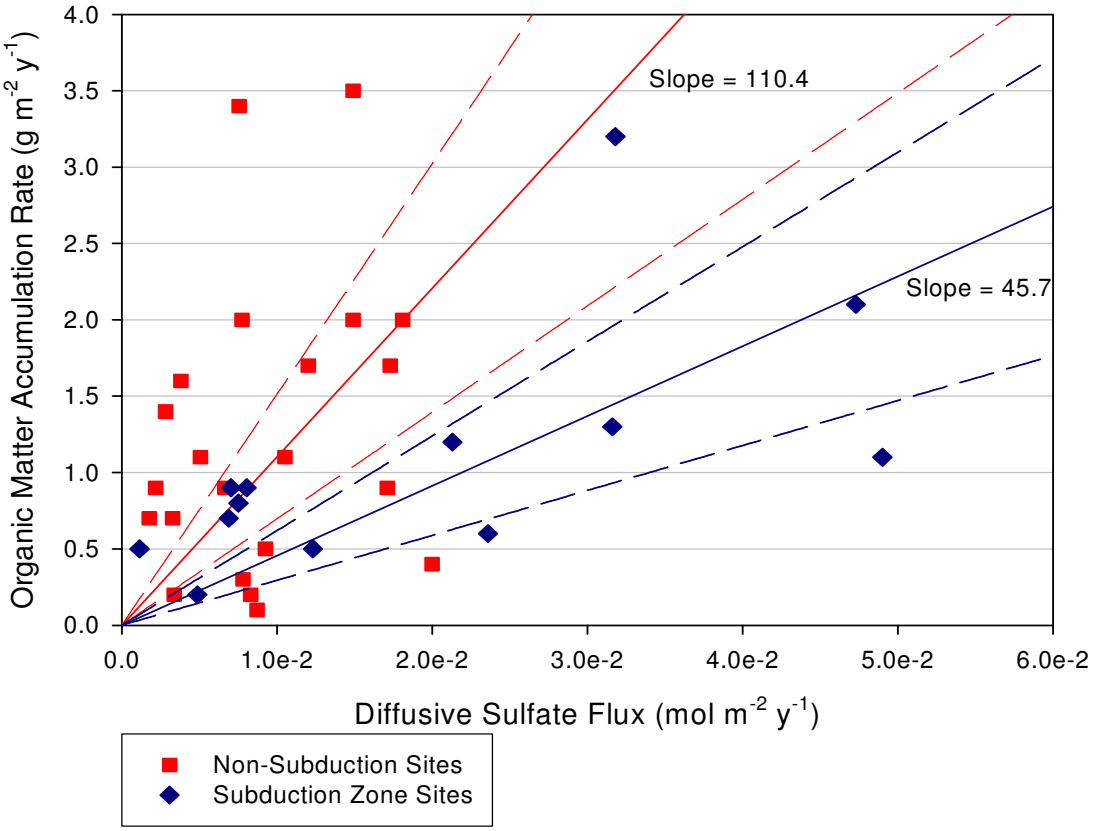

Figure 1.3b. Regression plot (solid lines), with 95% confidence intervals (dashed lines), showing how diffusive sulfate flux increases with increasing organic carbon accumulation rate at subduction zone sites and non-subduction margin sites. Same plot as Figure 1.3a, but with a shorter range of accumulation rates. See tables 1.3 and 1.4 for site locations and descriptions.

Due to the microbial ecological succession down the sediment column, methanogenesis is less prevalent above the SMTZ, and methane does not accumulate (Martens and Berner, 1974). So, additional methane to drive AOM must originate from below the SMTZ. At sites with diffusional regimes, the increased methane flux is most likely due to an increased methane concentration gradient. At diffusional sites with similar organic matter accumulation rates and reactivities, and thus similar *in situ* methane production in the sediments, the only way to increase the methane flux from

below the SMTZ is to transport methane-rich fluid to some point below the SMTZ, which would then allow methane to diffuse towards the SMTZ, creating a greater concentration gradient, driving a greater upward diffusional flux of methane.

A greater occurrence of tectonic uplift and deformation of sediments at subduction zone margins could be one cause of the greater diffusional methane flux. Uplift and deformation of continental slope sediments are more common at subduction zones than non-subduction margins due to the accretion of sediments from the oceanic plate and the stresses of involved in subduction (Kennett, 1982). If uplifting continental margin sediment has a methane profile which increases from the SMTZ downward, methane in deep porewater may become super-saturated due to the drop in pressure and form gaseous methane, as was proposed for Hydrate Ridge by Claypool et al., (2006). This gas could then rise through the lower sediment column, eventually dissolving in under-saturated porewater at some depth below the SMTZ. The dissolution of the methane in the porewater above would increase the methane concentration gradient and drive a greater methane flux to the SMTZ.

Also more common at subduction zone margins than at non-subduction convergent margins and divergent margins, is fluid flow along faults in the sediment (e.g., Schlüter, 2002). Thrust faults commonly form at subduction zones, along which fluid flows from below due to lateral compression and sediment compaction (Suess, 1985, Le Pichon, 1990, Moore and Vrolijk, 1992). With a downward increasing methane concentration profile, the fluid that flows from below is methane-rich relative to porewater above. With a fault running at some depth under the SMTZ, the fluid

moving along the fault would act as a source from which methane diffuses into surrounding sediments, increasing the methane concentration gradient, driving a greater diffusional flux of methane to the SMTZ.

Thus, increased fluid flow along faults in subduction zone sediments not only increases advective methane flux into surface sediments and ocean waters (e.g., Schlüter, 2002), but may also be shown to increase the diffusive flux of methane to overlying sediments, resulting in increased diffusive sulfate flux into the sediments.

1.6.3 Qualitative "High-Flux" Sites

Sites for which there are not at least three concentration measurements above the SMTZ cannot be used to quantify sulfate fluxes with reasonable uncertainty. Sites with SMTZ's at shallow depths relative to the sampling interval often do not have three measurements above the SMTZ. However, as long as the site data meet all other criteria for high-quality (see section 2.3.3), the site data can still be used to qualitatively determine whether they follow the same patterns of increasing diffusive sulfate flux with increasing organic carbon accumulation rate.

Though the exact SMTZ depth cannot be determined, the depth range in which the SMTZ is located can be found. The maximum depth of the SMTZ can be determined by the depth of the first measurement to reach background concentrations. Since sulfate concentrations reach background at the SMTZ, the shallowest point with background sulfate concentrations must be at or below the SMTZ. The SMTZ must, therefore, be between this first background point and the deepest non-background measurement above this point.

With few or no sulfate data above the SMTZ, the shape of the sulfate concentration profile to the SMTZ must be inferred. As shown in Figure 1.4, diffusive sulfate flux increases exponentially with decreasing SMTZ depth. Those sites with SMTZ depths less than about 15 meters have relatively high diffusive sulfate fluxes (Figure 1.4). All diffusional sites analyzed for this project which had calculable sulfate concentration gradients, and SMTZ's of 15 meters or less, had linear profiles, which is expected for sites with high fluxes. Based on this, it is assumed that all of these qualitative "high-flux" sites (Table 1.6) have linear profiles, and thus SMTZ depth is proportional to the diffusive sulfate flux, as shown in Figure 1.4.

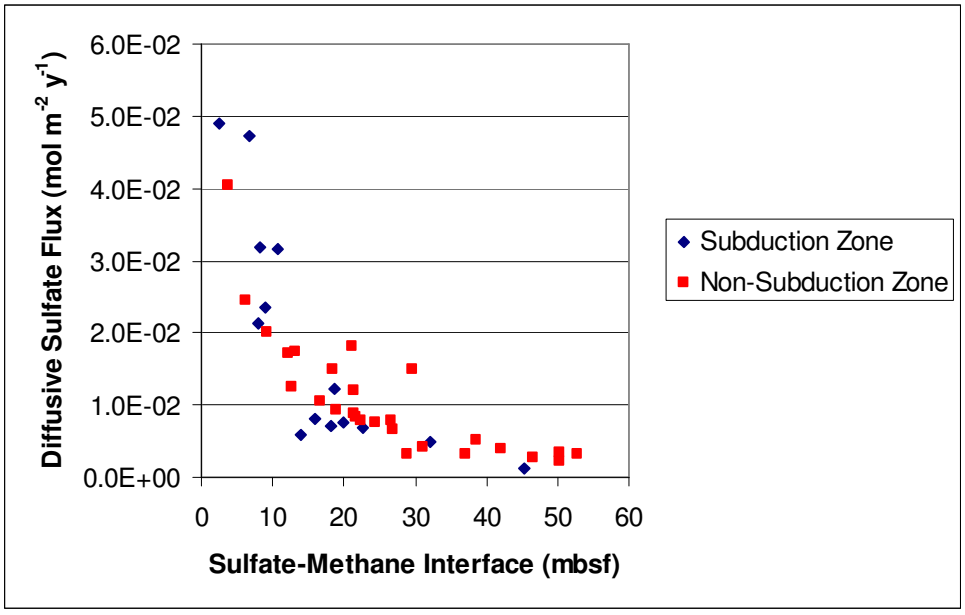

Figure 1.4. Plot showing how diffusive sulfate flux increases exponentially as SMTZ depth decreases.

Table 1.6. Qualitative "high-flux" site data.

Location	Leg	Site	Maximum SMTZ Depth (mbsf)	Minimum SMTZ Depth (mbsf)	Water Depth (m)	Porosity	Sedimentation Rate (cm ky^{-1})	Organic Carbon Accumulation Rate (g m^{-2} y^{-1})
Subduction Zone Sites								
Nankai	131	808	6.0	3.0	4675	0.66	90	5.3
Chile	141	859	5.0	0.0	2748	0.53	4	0.4
		860	7.5	6.0	2147	0.60	5	0.9
		861	7.5	0.0	1666	0.57	10	1.0
Cascadia	146	890	9.5	4.5	1326	0.62	6	0.3
	204	1246	7.5	3.0	850	0.64	31	4.8
		1250	5.0	0.0	795	0.63	15	2.1
Non-Subduction Margin Sites								
New Jersey	150	903	14.0	8.0	446	0.639	50	2.1
California	167	1019	12.5	4.5	980	0.65	22	2.1
W. Africa	175	1084	5.0	1.5	1992	0.827	27	6.7

When the ranges of possible SMTZ depth (maximum and minimum points connected by dashed lines in figure 1.5) are plotted against organic carbon accumulation rate (Figure 1.5), with SMTZ depth acting as a proxy for diffusive sulfate flux, the data show similar results as shown in Figure 1.3b. The diffusive sulfate flux is generally higher at subduction zone sites than non-subduction margin sites with similar or even somewhat greater organic carbon accumulation rates. Site 1084 from ODP Leg 175 may have an anomalously shallow SMTZ versus organic carbon accumulation rate for a non-subduction margin site because it has a much higher total organic carbon content; about 6% by weight, as compared with a range of between 0.4% and 1.6% for the other sites. While the results of Figure 1.5 may not be as clear as those in Figure 1.3b, they do act to generally support the hypothesis.

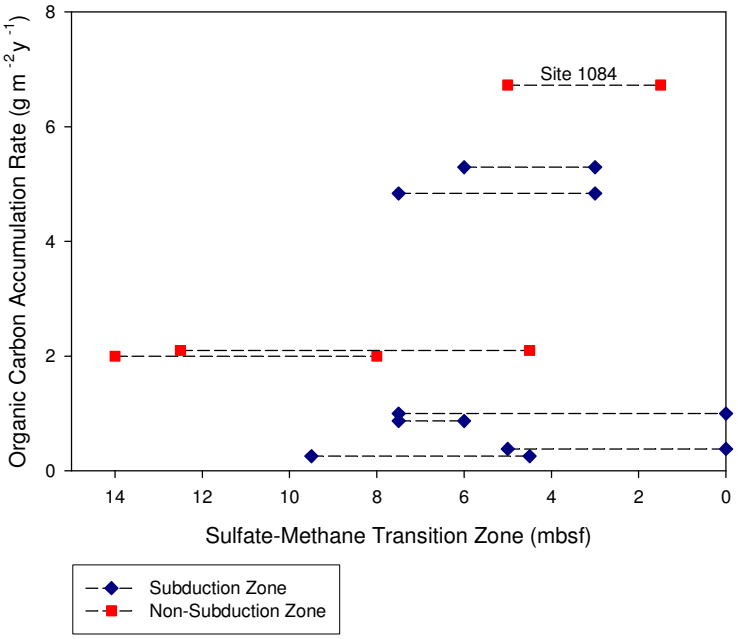

Figure 1.5. Plot shows decreasing SMTZ depth with increasing organic carbon accumulation rate. Horizontal dashed lines indicate depth intervals in which SMTZ's are located.

1.7 Conclusions

Subduction zone margin sediments exhibit higher diffusive methane fluxes to the SMTZ than non-subduction margin sediments with similar methane production rates. This has been interpreted as resulting from the advection of methane-rich fluids to some point below the SMTZ, which then drives a higher diffusive methane flux. The common difference between subduction zones versus other margins is the greater occurrence of deformation, faulting, and uplift of subduction zone sediments, which may cause greater fluid advection in the sediments.

The increased fluid flow in subduction zone sediments may be shown to increase the diffusive flux of methane to overlying sediments, resulting in increased diffusive sulfate flux into the sediments from overlying seawater.

1.8 References

Aller, R.C., 1982. The effects of macrobenthos on chemical properties of marine sediment and overlying water. In *Animal-Sediment Relations*. Editors McCall, P.L. and Tevesz, M.J.S., pp. 53-102, Plenum Press.

Archie, G.E., 1942. The electrical resistivity log as an aid in determining s reservoir characteristics. *Transactions of the American Institute of Mining, Metallurgical, and Petroleum Engineers,* **146**, 54–62.

Barnes, R.O. and Goldberg, E.D., 1976. Methane production and consumption in anoxic marine sediments. *Geology*, **4**, 297-300.

Bear, J., 1972. *Dynamics of Fluids in Porous Media*. Elsevier.

Berner, R.A., 1980. *Early Diagenesis- A Theoretical Approach*. Princeton University Press.

Boetius, A., Ravenschlag, K., Schubert, C.J., Rickert, D., Widdel, F., Gieseke, A., Amann, R., Jørgensen, B.B., Witte, U., Pfannkuche, O., 2000. A marine microbial consortium apparently mediating anaerobic oxidation of methane. *Nature,* **407**, 623-626.

Borowski, W.S., Paull, C.K., Ussler, W.U., 1996. Marine pore-water sulfate profiles indicate in situ methane flux from underlying gas hydrate. *Geology*, **24**(7), 655-658.

Borowski, W.S., Hoehler, T.M., Alperin, M.J., Rodriguez, N.M., Paull, C.K., 2000. Significance of anaerobic methane oxidation in methane-rich sediments overlying the Blake Ridge gas hydrates. In *Proceedings of the Ocean Drilling Program, Scientific Results*, Volume 164. Editors Paull, C.K., Matsumoto, R., Wallace, P.J., Dillon, W.P.

Claypool, G. E. and Kaplan, I.R., 1974. The origin and distribution of methane in marine sediments. In *Natural Gases in Marine Sediments.* Editor Kaplan, I.R., pp.99-139, Plenum.

Claypool, G.E., Milkov, A.V., Lee, Y.J., Torres, M.E., Borowski, W.S., Tomaru, H., 2006. Microbial methane generation and gas transport in shallow sediments of an accretionary complex, Southern Hydrate Ridge (ODP Leg 204), offshore Oregon, USA. In *Proceedings of the Ocean Drilling Program, Scientific Results* Volume 204. Editors Tréhu, A.M., Bohrmann, G., Torres, M.E., Colwell, F.S.

Cornell, D. and Katz, D.L., 1953. Flow of gases through consolidated porous media. *Industrial and Engineering Chemistry*, **45**, 2145-2152.

D'Hondt, S., Rutherford, S., Spivack, A.J., 2002. Metabolic activity of subsurface life in deep-sea sediments. *Science*, **295**, 2067-2070.

D'Hondt, S., Jørgensen, B.B., Miller, D.J., Batzke, A., Blake, R., Cragg, B.A., Cypionka, H., Dickens, G.R., Ferdelman, T., Hinrichs, K.U., Holm, N.G., Mitterer, R, Spivack, A., Wang, G., Bekins, B., Engelen, B., Ford, K., Gettemy, G., Rutherford, S.D., Sass, H., Skilbeck, C.G., Aiello, I.W., Guèrin, G., House, C.H., Inagaki, F., Meister, P., Naehr, T., Niitsuma, S., Parkes, R.J., Schippers, A., Smith, D.C., Teske, A., Wiegel, J., Padilla, C.N., Acosta, J.L., 2004. Distributions of microbial activities in deep subseafloor sediments. *Science,* **306**, 2216-2221.

Eganhouse, R.P. and Venkatesan, M.I., 1993. Chemical Oceanography and Geochemistry. In *Ecology of the Southern California Bight: A Synthesis and Interpretation*. Editors Dailey, M.D., Reish, D.J., and Anderson, J.W., University of California Press.

Gieskes, J.M., 1981. Deep-sea drilling interstitial water studies: Implications for chemical alteration of the oceanic crust, layers I and II. In *The Deep Sea Drilling Project: A Decade of Progress.* Editors Warme, J.E., Douglas, R.G., and Winterer, E.L., pp.149-167, Society of Economic Paleontologist and Mineralogists.

Hansen, L.B., Finster, K., Fossing, H., Iversen, N., 1998. Anaerobic methane oxidation in sulfate depleted sediments: effects of sulfate and molybdate additions. *Aquatic Microbial Ecology,* **14**, 195– 204.

Hedges, J.I. and Keil, R.G., 1995. Sedimentary organic matter preservation: an assessment and speculative synthesis. *Marine Chemistry*, **49**, 81-115.

Hensen, C., Zabel, M., Pfeifer, K., Schwenk, T., Kasten, S., Riedinger, N., Schulz, H.D., Boetius, A., 2003. Control of sulfate pore-water profiles by sedimentary events and the significance of anaerobic oxidation of methane for the burial of sulfur in marine sediments. *Geochimica et Cosmochemica Acta,* **67**, 2631-2647.

Hinrichs, K.U., Hayes, J.M., Sylva, S.P., Brewer, P.G., DeLong, E.F., 1999. Methane-consuming archaebacteria in marine sediments. *Nature,* **398**, 802– 805.

Hoehler, T.M., Alperin, M.J., Albert, D.B., Martens, C.S., 1994. Field and laboratory studies of methane oxidation in an anoxic marine sediment: Evidence for a methanogenic-sulfate reducer consortium. *Global Biogeochemical Cycles,* **8**, 451–463.

Horne, R.A., Day, A.F., Young, R.P., 1969. Ionic diffusion under high pressure in porous solid materials permeated with aqueous, electrolytic solution. Journal of Physical Chemistry, **73**, 2782.

Froelich, P.N., Klinkhammer, G.P., Bender, M.L., Luedtke, N.A., Cullen, D., Duaphin, P., 1979. Early oxidation of organic matter in pelagic sediments of the eastern equatorial Atlantic: suboxic diagenesis. *Geochimica et Cosmochemica Acta,* **43**, 1075-1090.

Kennett, J.P., 1982. *Marine Geology*. Prentice-Hall, Inc.

Li, Y., and Gregory, S., 1974. Diffusion of ions in sea water and in deep-sea sediments: *Geochimica et Cosmochimica Acta*, **38**, 703–714.

McDuff, R.E. and Ellis, R.A., 1979. Determining diffusion coefficients in marine sediments: A laboratory study of the validity of resistivity techniques. *American Journal of Science*, **279**, 666-675.

Reeburgh, W.S., 1976. Methane consumption in Cariaco Trench waters and sediments. *Earth and Planetary Science Letters*, **28**, 337-344.

Reeburgh, W.S., 2007. Oceanic methane biogeochemistry. *Chemical Reviews*, **107**(2), 486-513.

Schlunz, B., Schnieder, R.R., Muller, P.J., Showers, W.J., Wefer, G., 1999. Terrestrial organic carbon accumulation on the Amazon deep sea fan during the last glacial sea level low stand. *Chemical Geology*, **159**, 263-281.

Schlüter, M., 2002. Fluid flow in continental margin sediments. In *Ocean Margin Systems*. Editors Wefer, G., Billet, D., Hebbeln, D., Jorgensen, B.B., Schlüter, M., Van Weering, T. pp. 205-217.

Ullman, W.J. and Aller, R.C., 1982. Diffusion coefficients in nearshore marine sediments. *Limnology and Oceanography*, **27**, 552-556.

Whiticar, M.J., 1999. Carbon and hydrogen isotope systematics of bacterial formation and oxidation of methane. *Chemical Geology*, **161**, 291-314.

CHAPTER 2

Depositional Constraints on Formation Factor Estimates

2.1 Abstract

In the absence of measured formation factors of sediment cores, it is necessary to determine effective estimates for formation factor values using other measured properties of the sediment. Using data collected from the Ocean Drilling Program (ODP), the relationship between average porosity and average formation factor is determined for sediments from several depositional environments and with several lithologies. Average values of porosity and formation factor are generally utilized for the calculation of chemical flux through saturated sediment. So that the results of this study may be of practical use when calculating chemical fluxes using linear concentration gradients, average values of formation factor and porosity are used from depths between the seafloor and 50 meters depth. The relationship between porosity and formation factor can be more precisely estimated when both the lithology and depositional environment are taken into account. It is suggested that this compilation could be used as a guide for assigning values of the Archie exponent based on sediment depositional environment and lithology for sites for which formation factor data are not available.

2.2 Introduction

Since Archie's 1942 paper, several alternative formulas have been proposed to estimate the relationship between formation factor and porosity for various sediment types. These formulas can be divided into three groups based on the number of

adjustable constants in the relationship, the first group having none, the second group containing one, and the third group containing multiple constants. The formulas containing no adjustable constants, based on theoretical pore geometries, were evaluated (Boudreau, 1996) and found to be poor fits to measured values from fine-grained sediment compared with empirical formulas containing one adjustable parameter.

These empirical formulas that fit to measured values of formation factor and porosity using one adjustable parameter (Table 2.1), were also compared with each other, and shown to have different precisions at different porosity ranges for fine-grained sediments (Boudreau, 1996). The equation advanced by Iversen and Jorgensen (1993), compared with Archie's formula, is proposed to be a more precise fit to sediments with porosities between 0.40 and 0.85, with n=3 for clay-silt sediments, and n=2 for sandy sediments (Iversen and Jorgensen, 1993). The equation proposed by Boudreau (1996), is demonstrated to be similarly precise as the Iversen and Jorgensen equation for fine-grained sediments with porosities between 0.40 and 0.85, and more precise for fine-grained sediments with observed porosity values outside of that range; from about 0.30-0.40 and 0.85-0.95 (Boudreau, 1996).

Table 2.1. Equations relating formation factor and porosity which utilize a single adjustable constant. F is formation factor, φ is porosity, and n is the adjustable constant. Formula #'s are referenced in Tables 2.4 and 2.5.

#	Formula	Sources
2.1	$F = \varphi^{-n}$	Archie, 1942
2.2	$\varphi F = 1 + n(1 - \varphi)$	Iversen and Jorgensen, 1993; Low, 1981
2.3	$\varphi F = 1 - \ln(\varphi^n)$	Boudreau, 1996; Weissberg, 1963

Using the equation proposed by Atkins and Smith (1961):

$$F = a\varphi^{-n} \quad (2.4)$$

where (F) is formation factor, (φ) is porosity, and (a) and (n) are both adjustable constants, a more precise fit may be made to the data over a wider porosity range by varying both (a) and (n) for each sediment lithology (Atkins and Smith, 1961; Turk, 1976). However, approximation using just one adjustable constant is thought to be adequate (Ullman and Aller, 1982; Iversen and Jorgensen, 1993), taking into account the realistic precision of a model based on properties of natural sediments. Also, if the value of the parameter (a) is not 1, the model proposed by Atkins and Smith, (1961) does not satisfy the theoretical requirement that the formation factor be equal to 1 when the porosity has a (theoretical) value of 1 (see section 1.3.3.2).

The precisions of the single variable formulas are evaluated using sediments categorized by lithology and depositional environment to determine which formula can most precisely model natural sediments. Previous studies use formation factor and porosity data that are categorized by lithology alone. In this chapter, measured formation factor and porosity data from the ODP are categorized by both lithology and depositional environment in order to determine whether depositional environment has an effect on the pore structure of the sediment, independent of lithology.

2.3 Methodology

2.3.1 Collection of Data

Formation factor and porosity data were collected from the Integrated Ocean Drilling Program (IODP) online database and the Initial Reports of the Ocean Drilling

Program (ODP) for every ODP and IODP site for which both formation factors and porosities have been measured. Following formula 2.1 (see Table 2.1), where (F) is the formation factor and (φ) is the porosity, the value of the exponent (n) is calculated for each site which has high-quality, published formation factor and porosity data. These sites are categorized by depositional environment: continental shelf, continental slope, continental margin plateau, deep ocean basin, and deep sea topographic ridge; and lithology: mud, sand, calcareous ooze, siliceous ooze.

2.3.2 Consistency between Depth Intervals

In order to ensure that the relationship between average formation factor and average porosity is consistent for a given environment and sediment type over a range of depth intervals, average values of the formation factors and porosities are calculated for the top 10 meters and the top 50 meters of each site. Out of all ODP and IODP sites with linear, diffusional sulfate concentration gradients due to the anaerobic oxidation of methane (AOM), the maximum depth at which sulfate concentration reaches background levels, commonly known as the sulfate-methane transition zone (SMTZ), is 53 meters and the shallowest is 2.4 meters (Figure 2.1). Thus, the 10 meter and 50 meter depth intervals cover both the shallow and deep depths of relevancy to the calculation of sulfate fluxes from linear concentration gradients.

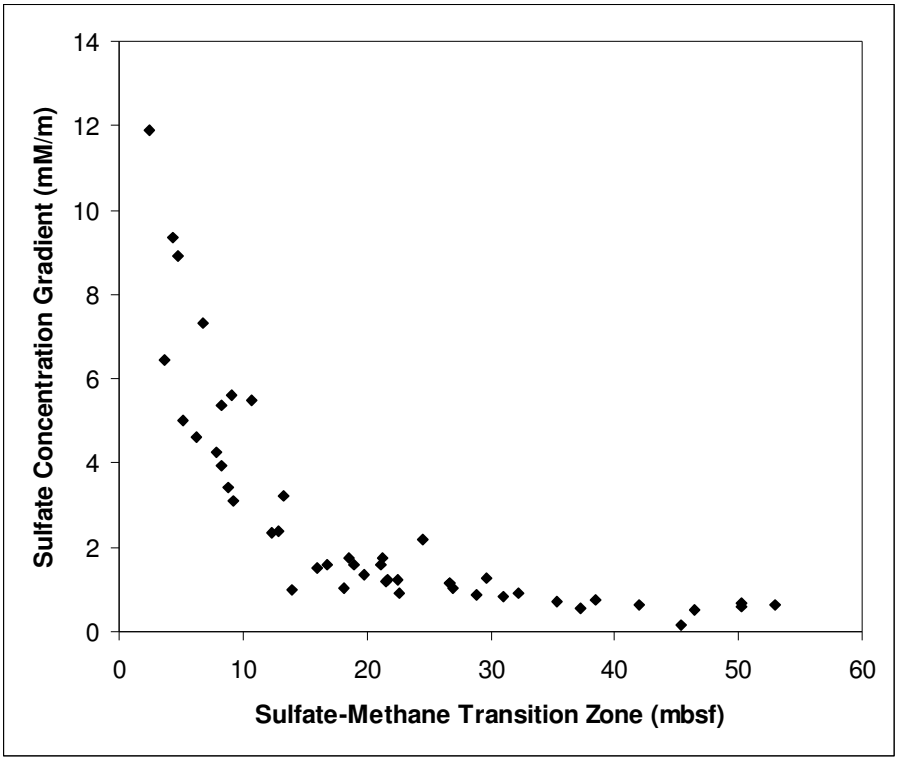

Figure 2.1. Plot of sulfate-methane transition zone (SMTZ) depth versus linear sulfate concentration gradient. Data from ODP and IODP (see section 1.5).

2.3.3 Data Quality

Averages of porosity and formation factor are calculated for the depth intervals of about 0-10 mbsf and 0-50 mbsf, the exact depth interval being dependent on available data. For the 0-10 mbsf interval, the measured formation factor data has to meet the following criteria: (a) there is no measurement gap greater than 3 meters between 0 and 10 mbsf, (b) the formation factor must have a value greater than 1, and (c) the deepest measurement is at 10 mbsf or at greater depth, unless it does not meet criterion (a), in which case the deepest measurement less than 10 mbsf is used as the deep end-member. For the 0-50 mbsf interval, the measured formation factor data has to meet the following criteria: (a) there is no measurement gap greater than 15 meters

between 0 and 50 mbsf, (b) the formation factor must have a value greater than 1, and (c) the deepest measurement is at 50 mbsf or at greater depth, unless it does not meet criterion (a), in which case the deepest measurement above 50 mbsf is used as the deep end-member. Criterion (b) is necessary because formation factor values below 1 are not physically reasonable in sediment that is less conductive than the interstitial water (see Section 1.3.3.2). Thus, no data are used from any expedition which recorded formation factors less than 1. Porosity measurements that most closely match the depth of the formation factor measurements are selected. The porosity measurements chosen are required to be within one meter of the formation factor measurement. The great majority of the formation factors are matched with porosities from similar depths, within a few centimeters.

2.3.4 Calculation of Averages

Since porosity and formation factor are physical properties of the sediment and the depth intervals between measurements are not always equal, a simple arithmetic average is not adequate. The method used to average the physical properties of the sediment has to assign weight to each individual value based on the depth interval it represents and has to account for the physical transition from one value to another. In order to account for these factors, a graphical approach is used to calculate the average porosities and formation factors of the sediment. First, the values are plotted versus depth as a scatter plot with the points connected by straight lines, which represents a core in which the values of the physical properties transition linearly from one measured value to the next. The area under the curve is then calculated using the

SigmaPlot function “Area Below Curves”, which uses the trapezoidal rule to integrate the line. Dividing the area by the total depth interval gives an average value of the porosity or formation factor of the sediment column.

2.3.5 Depositional Environments

The seafloor environment of each site was obtained from the Site Reports in the Initial Reports of the Proceedings of the Ocean Drilling Program, and cross-referenced with water depth, seafloor topographic maps and, in ambiguous cases, the seismic profiles of the site locations. Though the continental shelf, slope, and rise are defined by gradient, for this study, a site is categorized as being on a continental shelf environment if it lies on a continental margin at a water depth of 200 meters or less. For this study, a continental slope environment is considered to be on the continental margin, below the above defined shelf, and above the topographically distinct continental rise and deep-ocean basin environments, which are distinguished in cross-section. Deep-ocean basin environments are distinguished by their near lack of inclination and are generally the deepest area of an ocean other than the trenches. The deep-ocean basin category may contain some continental rise sites. Continental margin plateaus are defined as flat, broad continental margins which are deeper than the shelf environment. All of the margin plateau environments in this study are from the Queensland Plateau area on the north-east margin of Australia and the Exmouth Plateau on the north-west margin of Australia. Topographic deep-sea ridges are defined as aseismic ridges located within an ocean basin environment.

The depositional environments of the sites are separated into five categories based on the water depth and topography, which affect the stability of sediment (Kennett, 1982). These categories, defined above, are: continental shelf, continental margin plateau, continental slope, deep-ocean basin, and topographic deep-sea ridge. Sediment in the shelf environment is significantly affected by wave action, currents, and other fluid movement along the seafloor. The margin plateaus are flat, gravitationally stable environments which, at the sites in this study, receive almost exclusively pelagic sediment. The slope is topographically more unstable than other environments; it is more prone to gravity-driven flows of material. The basins are nearly flat, stable environments, which may receive some material from the larger gravity flows off the slope, but mostly pelagic sediment is deposited there. Topographic deep-sea ridges are gravitationally less stable than deep ocean basins due to the topography, but are located in deep water with low sedimentation rates which make them more stable than continental margin slopes.

2.3.6 Lithologies

The lithologies are separated into major and minor lithology for each site. The lithologies represent averages from the respective depth interval of sediment (either 10 meters or 50 meters) as it is described in the Site Reports of the Initial Reports of the Proceedings of the Ocean Drilling Program. The sediment types were categorized as nanofossil ooze, foraminiferal ooze, siliceous ooze, clay, silt, or sand. Nanofossil and foraminiferal oozes were then combined into one calcareous ooze category, and clay and silt were combined into a single mud category, since no significant differences

were present in the porosities, formation factors, or Archie exponent values of these similar sediment types.

2.3.7 Water Depth

The water depth of each site is the depth of the seafloor from sea level, which were obtained from the IODP online database.

2.4 Sites

For the interval from 0-10 mbsf, a total of 31 sites from 8 drilling legs (Table 2.2) meet the criteria, and for the interval from 0-50 mbsf, a total of 47 sites from 9 drilling legs (Table 2.3) meet the criteria.

Table 2.2. ODP site data for 0-10 mbsf depth interval. Lithology abbreviations: calc.: calcareous ooze, sili.: siliceous ooze. Blank fields under "Minor Lithology" indicate no minor lithologies. The "Exponent" refers to the exponent (n) in Eqn. 2.1.

ODP Leg	Site	Water Depth (mbsl)	Environment	Major Lithology	Minor Lithology	Average Porosity (%)	Average Formation Factor	Archie Formula Exponent
127	794	2811	basin	mud		80.8	1.90	3.01
	795	3300	basin	mud		82.9	1.98	3.64
	796	2570	ridge flank	mud	sili.	76.6	2.55	3.51
	797	2862	basin	mud		83.2	1.70	2.89
133	813	539	margin plateau	calc.		67.2	1.90	1.61
	814	520	margin plateau	calc.		66.3	2.40	2.13
	815	466	slope	calc.		59.8	3.37	2.36
	816	438	slope	calc.	mud	61.9	3.79	2.78
	817	1017	slope	calc.		65.1	3.29	2.77
	818	745	slope	calc.		63.4	2.84	2.29
	819	565	slope	calc.	mud	63.2	3.32	2.62
	820	278	slope	mud	sand	61.2	2.63	1.97
	821	213	slope	sand	mud	59.1	3.33	2.29
	822	955	slope	calc.	mud	61.9	3.38	2.54
146	890	1326	slope	mud		60.3	3.20	2.30
	891	2663	slope	mud	sand	50.3	4.32	2.13
168	1023	2593	basin	mud		67.3	2.34	2.15
	1025	2606	basin	mud		69.1	1.65	1.35
	1028	2659	basin	mud	sand	62.0	1.65	1.05
	1031	2588	basin	mud		72.9	3.40	3.87
170	1040	4177	slope	mud	sand	55.1	2.95	1.82
	1043	4313	slope	mud	breccia	65.1	2.11	1.74
172	1056	2167	slope	mud	calc.	66.0	2.83	2.50
	1057	2584	slope	mud	calc.	68.9	2.88	2.84
	1058	2985	slope	mud		68.1	2.31	2.18
	1060	3481	slope	mud	calc.	76.2	2.51	3.39
190	1174	4751	slope	mud		64.4	3.22	2.66
201	1225	3761	basin	sili.	calc.	76.7	2.06	2.72
	1226	3297	basin	sili.	calc.	82.0	2.08	3.69
	1227	428	slope	sili.		73.1	2.92	3.42
	1229	152	shelf	mud		78.6	2.34	3.53

Table 2.3. ODP site data for 0-50 mbsf depth interval. Lithology abbreviations: calc.: calcareous ooze, sili.: siliceous ooze. Blank fields under "Minor Lithology" indicate no minor lithologies. The "Exponent" refers to the exponent (n) in Eqn. 2.1.

ODP Leg	Site	Water Depth (mbsl)	Environment	Major Lithology	Minor Lithology	Average Porosity (%)	Average Formation Factor	Archie Formula Exponent
121	752	1086	ridge crest	calc.		65.0	2.11	1.73
	753	1176	ridge flank	calc.		64.2	2.00	1.56
	754	1064	ridge crest	calc.		63.0	1.98	1.48
	756	1518	ridge crest	calc.		59.5	1.55	0.84
	757	1650	ridge crest	calc.		63.6	1.68	1.15
	758	2925	ridge flank	calc.	mud	69.0	1.55	1.18
122	760	1970	margin plateau	calc.		64.0	2.49	2.04
	762	1360	margin plateau	calc.		65.5	2.45	2.12
	763	1368	margin plateau	calc.		66.5	2.64	2.38
127	794	2811	basin	mud	sili.	77.6	2.09	2.91
	795	3300	basin	mud	sili.	80.2	2.16	3.49
	796	2570	ridge flank	mud	sili.	73.8	3.05	3.67
	797	2862	basin	mud		80.7	1.88	2.94
133	811	937	margin plateau	calc.		62.8	2.62	2.07
	813	539	margin plateau	calc.		67.1	2.24	2.02
	814	520	margin plateau	calc.		64.6	2.25	1.86
	815	466	slope	calc.	mud	60.5	3.32	2.39
	816	438	slope	calc.	mud	59.8	3.54	2.46
	817	1017	slope	calc.		64.4	3.02	2.51
	818	745	slope	calc.		61.3	2.74	2.06
	819	565	slope	calc.	mud	56.8	4.39	2.62
	820	278	slope	mud	sand	56.5	3.04	1.95
	821	213	slope	sand	mud	56.1	3.68	2.25
	822	955	slope	calc.	mud	57.2	4.09	2.52
168	1023	2593	basin	mud	sand	63.7	2.57	2.09
	1025	2606	basin	mud	sand	64.5	2.16	1.76
	1026	2658	basin	mud	sand	58.7	2.77	1.91
	1027	2657	basin	mud	sand	60.9	2.82	2.09
	1028	2659	basin	mud	sand	62.2	1.52	0.88
	1029	2653	basin	sand	mud	61.9	3.19	2.42
	1030	2574	basin	mud		68.2	2.96	2.84
	1031	2588	basin	mud		73.2	3.62	4.12
170	1043	4313	slope	mud	breccia	58.4	3.22	2.17
172	1055	1799	slope	mud	calc.	63.1	3.78	2.89
	1056	2167	slope	mud	calc.	64.2	3.99	3.12
	1057	2584	slope	mud	calc.	65.0	3.99	3.21
	1058	2985	slope	mud	calc.	64.9	3.22	2.70
	1060	3481	slope	mud	calc.	72.0	3.48	3.80
	1061	4047	slope	mud	calc.	71.2	3.34	3.55
	1062	4763	basin	mud	calc.	72.7	2.78	3.21

Table 2.3 (cont.). ODP site data for 0-50 mbsf depth interval. Lithology abbreviations: calc.: calcareous ooze, sili.: siliceous ooze. Blank fields under "Minor Lithology" indicate no minor lithologies. The "Exponent" refers to the exponent (n) in Eqn. 2.1.

ODP Leg	Site	Water Depth (mbsl)	Environment	Major Lithology	Minor Lithology	Average Porosity (%)	Average Formation Factor	Archie Formula Exponent
190	1174	4751	slope	sand	mud	61.2	3.70	2.66
	1175	2998	slope	mud	a	65.4	3.30	2.81
	1176	3021	slope	mud	sand	68.7	2.78	2.72
201	1225	3761	basin	calc.	sili.	77.7	2.07	2.88
	1226	3297	basin	calc.	sili.	79.6	2.10	3.25
	1227	428	slope	mud	sili.	73.0	2.64	3.08
	1229	152	shelf	sili.	mud	73.5	2.53	3.01

The selected sites are from the following ODP drilling legs: ODP Leg 121 drilled the Broken Ridge and Ninetyeast Ridge in the Indian Ocean. ODP Leg 122 drilled the Exmouth Plateau off the north-east coast of Australia. ODP Leg 127 drilled in the Japan Sea. ODP Leg 131 drilled the margin off the south-east coast of Japan in the Nankai Trough. ODP Leg 133 drilled the continental margin off the north-east coast of Australia. ODP Leg 146 drilled the Cascadia margin off the coast of the Pacific Northwest United States. ODP Leg 168 drilled near the Juan de Fuca Ridge in the north-east Pacific Ocean. ODP Leg 170 drilled the margin off the western shore of Costa Rica. ODP Leg 172 drilled the Blake Ridge and Bahama Rise off the East Coast United States. ODP Leg 190 drilled the margin off the south-east coast of Japan in the Nankai Trough, near the ODP Leg 131 site. ODP Leg 201 drilled the continental margin off the coast of Peru.

With only one continental shelf site (Leg 201, Site 1229) having available high-quality data for calculation of average porosity and formation factor, the

relationship between the two properties for the shelf environment cannot be adequately determined and is not discussed below.

2.5 Results and Discussion

2.5.1 Formula Comparison

2.5.1.1 Determination of Uncertainty

Porosity and formation factor values of sediments categorized by depositional environment and lithology are plotted (Figures 2.2-2.7) with Archie's formula and the formulas put forward by Boudreau, (1996) and Iversen and Jorgensen, (1993) in order to determine which formula has the least uncertainty when estimating formation factor values of sediments with measured porosities.

The maximum scatter in the data between different values of the adjustable constant in each formula is estimated from the plots. Assuming the maximum scatter of the data represents the range of adjustable constant values for that particular lithology and depositional environment, the scatter can be used as the uncertainty of the adjustable constant estimation. The scatter in the values of adjustable constants for the formulas of Iversen and Jorgensen, (1993), and Boudreau, (1996) are approximated for the interval of about 0.50-0.85. However, for Archie's formula, differentiation between two porosity ranges is needed since Ullman and Aller, (1982) observe that, using Archie's relationship, sediments with porosity greater than 0.70 have an exponent value 0.5-1.0 greater than sediments of similar lithology with lower porosities. So, for Archie's formula, the scatter of those points with porosities of 0.50-

0.70 is determined separately from those with porosities of 0.70-0.85. The values for the scatter are approximated using at least three data points.

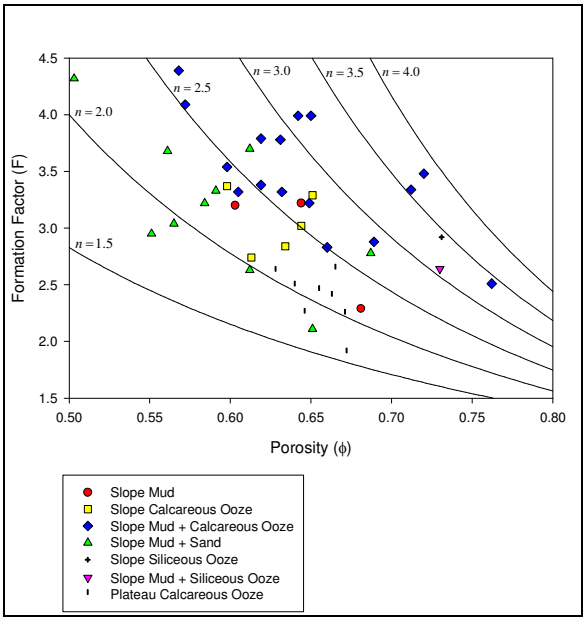

Figure 2.2. Plot of continental margin data showing Archie formula trend lines with exponent (n) values between 1.5 and 4.0.

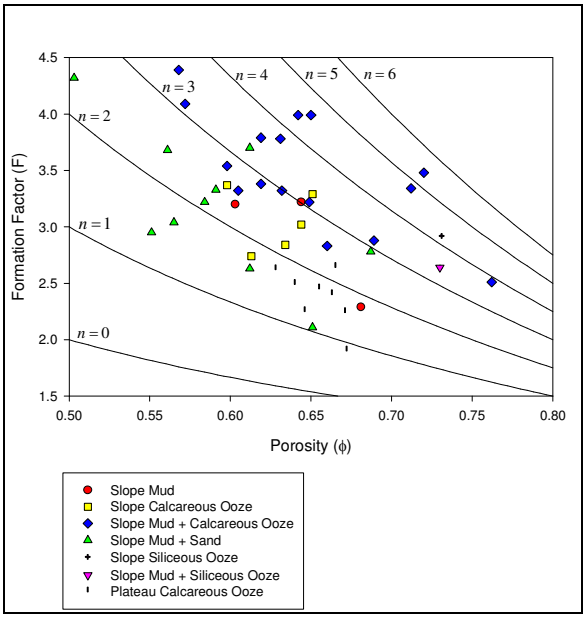

Figure 2.3. Plot of continental margin data showing trend lines of formula used by Iversen and Jorgensen, (1993), with (n) values between 0 and 6.

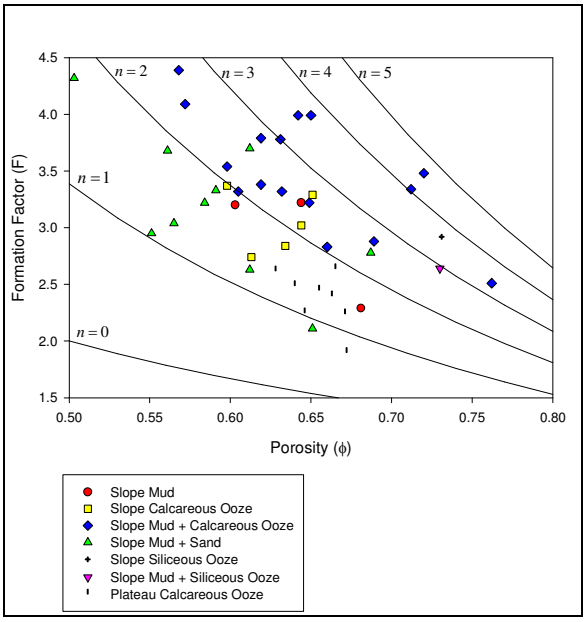

Figure 2.4. Plot of continental margin data showing Boudreau, (1996), formula trend lines with (n) values between 0 and 5.

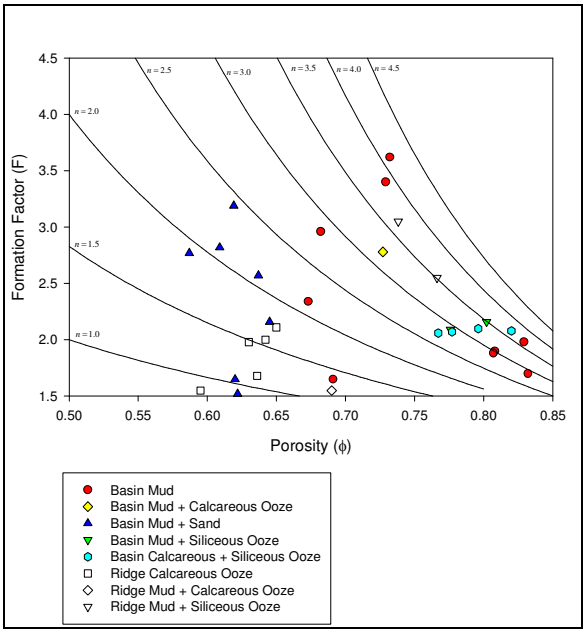

Figure 2.5. Plot of deep ocean basin and ridge data showing Archie formula trend lines with exponent (n) values between 1.0 and 4.5.

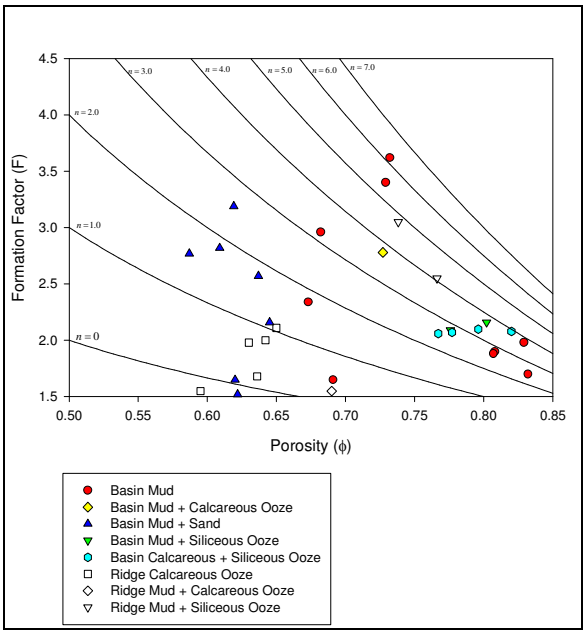

Figure 2.6. Plot of deep ocean basin and ridge data showing trend lines of formula used by Iversen and Jorgensen, (1993), with (n) values between 0 and 7.

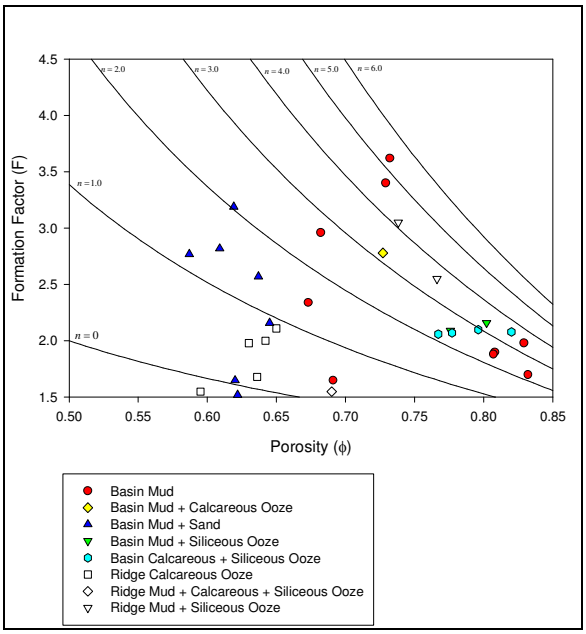

Figure 2.7. Plot of deep ocean basin and ridge data showing Boudreau, (1996), formula trend lines with (n) values between 0 and 6.

Since each formula is different, comparing uncertainties in the adjustable constants of each formula would have no meaning. That is, the uncertainties in the adjustable constants cannot be directly compared in order to compare the uncertainties of the formulas. Instead, the relative uncertainty in the formation factor at a given porosity due to the uncertainty in adjustable constant value must be calculated for each formula and compared to determine which formula is most precise (Tables 2.4 and 2.5).

With a constant uncertainty in the value of the adjustable constant, the uncertainty of the formation factor increases with decreasing porosity for all three formulas. Using constant uncertainties in the values of the adjustable constants, obtained from the data scatter, maximum and minimum relative uncertainties in the values of the formation factors are calculated for the porosity range between 0.50 and 0.70, with the maximum relative uncertainty being the relative uncertainty below the value of the adjustable constant at 0.50 porosity, and the minimum relative uncertainty being the uncertainty above the value of the adjustable constant at 0.70 porosity. If there are at least three data points at porosities above 0.70 for a given lithology and depositional environment, the scatter is also calculated for the porosity range of 0.70-0.85, with maximum and minimum relative uncertainties calculated in the same manner as above.

2.5.1.2 Continental Margin Sites

The most useful formula is the one which will have the least amount of uncertainty in the formation factor estimate throughout the porosity range of interest.

The uncertainty must be evaluated at both high and low porosities in order to determine the minimum and maximum uncertainties, respectively. The minimum and maximum uncertainties must be evaluated because the uncertainties change to different degrees through the porosity range between the three formulas. For the lithologies of the continental margins, Archie's formula and the Iversen and Jorgensen formula fit the ODP data best. The formula put forward by Boudreau does not fit the ODP data as well as the other two formulas for the porosity range of 0.50-0.85.

Archie's formula has the lowest maximum relative uncertainty for three of the six lithologies (mud + calcareous ooze with $\varphi > 0.70$, mud + sand, plateau calcareous ooze), and the lowest minimum relative uncertainty for four of the six lithologies (mud + calcareous ooze with $\varphi > 0.70$, mud + calcareous ooze with $\varphi < 0.70$, mud + sand, plateau calcareous ooze) listed in Table 2.4. The Iversen and Jorgensen formula has the lowest maximum relative uncertainty for four of the six lithologies (mud, slope calcareous ooze, mud + calcareous ooze with $\varphi < 0.70$, plateau calcareous ooze) and the lowest minimum relative uncertainty for three of the six lithologies listed (mud, slope calcareous ooze, mud + calcareous ooze with $\varphi < 0.70$). The Boudreau formula has the lowest maximum relative uncertainty for one of the six lithologies (mud + sand), and the lowest minimum relative uncertainty for none of the six lithologies listed.

Table 2.4. Analysis of continental margin data. Formula # refers to formulae in Table 1. Note adjustable constants are of differing formulae and should not be directly compared. Porosity range is the range for which formation factor uncertainty was calculated. Highlighted uncertainties are the lowest uncertainties for a particular lithologic category.

Formula #	Sediment Type	Depositional Environment	Adjustable Constant Value	Scatter (+/-)	Formation Factor Estimation		
					Porosity Range	Maximum Uncertainty (%)	Minimum Uncertainty (%)
1	Mud	Slope	2.5	0.5	0.50-0.70	29	20
2	Mud	Slope	2.5	1.0	0.50-0.70	22	17
3	Mud	Slope	2.0	1.0	0.50-0.70	29	21
1	Calcareous Ooze	Slope	2.5	0.5	0.50-0.70	29	20
2	Calcareous Ooze	Slope	2.5	1.0	0.50-0.70	22	17
3	Calcareous Ooze	Slope	2.0	1.0	0.50-0.70	29	21
1	Mud + Calcareous Ooze	Slope	2.75	0.5	0.50-0.70	29	20
2	Mud + Calcareous Ooze	Slope	4.0	1.5	0.50-0.70	25	20
3	Mud + Calcareous Ooze	Slope	3.5	1.5	0.50-0.70	30	24
1	Mud + Calcareous Ooze	Slope	3.5	0.5	0.70-0.85	16	8
2	Mud + Calcareous Ooze	Slope	4.0	1.5	0.70-0.85	20	14
3	Mud + Calcareous Ooze	Slope	3.5	1.5	0.70-0.85	24	12
1	Mud + Sand	Slope	2.25	0.5	0.50-0.70	29	20
2	Mud + Sand	Slope	2.0	1.5	0.50-0.70	38	28
3	Mud + Sand	Slope	2.0	1.0	0.50-0.70	29	21
1	Calcareous Ooze	Plateau	2.0	0.5	0.50-0.70	29	20
2	Calcareous Ooze	Plateau	1.5	1.0	0.50-0.70	29	21
3	Calcareous Ooze	Plateau	1.5	1.0	0.50-0.70	34	23

2.5.1.3 Basin and Ridge Sites

Archie's formula and the Iversen and Jorgensen formula both also fit the data best for the lithologies of the Basins and Ridges, though Archie's formula has the least uncertainty for most of the lithologies. Archie's formula has the lowest maximum relative uncertainty for four of the five lithologies (mud with φ <0.70, mud with φ >0.70, mud + sand, calcareous ooze), and the lowest minimum relative uncertainty for three of the five lithologies (mud with φ <0.70, mud with φ >0.70, calcareous ooze) listed in Table 2.5. The Iversen and Jorgensen formula has the lowest maximum relative uncertainty for two of the five lithologies (mud + sand, calcareous + siliceous ooze), and the lowest minimum relative uncertainty for two of the five lithologies listed (mud + sand, calcareous + siliceous ooze). The Boudreau formula has the lowest maximum relative uncertainty for none of the five lithologies, and the lowest minimum relative uncertainty for one of the five lithologies listed (mud with φ <0.70).

Table 2.5. Analysis of deep ocean basin and ridge data. Formula # refers to formulae in Table 1. Note adjustable constants are of differing formulae and should not be directly compared. Porosity range is the range for which formation factor uncertainty was calculated. Highlighted uncertainties are the lowest uncertainties for a particular lithologic category.

Formula #	Sediment Type	Depositional Environment	Adjustable Constant Value	Scatter (+/-)	Formation Factor Estimation		
					Porosity Range	Maximum Uncertainty (%)	Minimum Uncertainty (%)
1	Mud	Basin	2.0	1.0	0.50-0.70	50	43
2	Mud	Basin	3.5	3.0	0.50-0.70	55	44
3	Mud	Basin	3.0	2.5	0.50-0.70	56	43
1	Mud	Basin	3.5	1.0	0.70-0.85	30	18
2	Mud	Basin	3.5	3.0	0.70-0.85	44	30
3	Mud	Basin	3.0	2.5	0.70-0.85	43	27
1	Mud + Sand	Basin	1.5	1.0	0.50-0.70	50	43
2	Mud + Sand	Basin	1.0	1.5	0.50-0.70	50	35
3	Mud + Sand	Basin	1.0	1.5	0.50-0.70	61	39
1	Calcareous + Siliceous Ooze	Basin	3.25	1.0	0.70-0.85	30	18
2	Calcareous + Siliceous Ooze	Basin	3.0	1.0	0.70-0.85	16	10
3	Calcareous + Siliceous Ooze	Basin	3.0	1.0	0.70-0.85	17	11
1	Calcareous Ooze	Ridge	1.25	0.5	0.50-0.70	29	20
2	Calcareous Ooze	Ridge	0.5	1.0	0.50-0.70	40	26
3	Calcareous Ooze	Ridge	0.5	1.0	0.50-0.70	51	30

Archie's formula and the formula put forward by Iversen and Jorgensen can be used with similar precision for continental margin lithologies with porosities between 0.50-0.85, and Archie's formula is the better choice for the deep-ocean basin and deep-sea topographic ridge lithologies listed with porosities between 0.50-0.85. Archie's formula is also the simplest formula of the three and will be the formula used to demonstrate that depositional environment has an effect on pore structure and that the value of the adjustable constant doesn't significantly change with depth in the top 50 meters of sediment.

2.5.2 Effect of Depositional Environment

The value of the exponent (n) in Archie's formula determines the change of the formation factor value with a change in porosity. The exponential relationship causes the rate of increase of the formation factor to increase as porosity decreases. Since formation factor is also equivalent to the tortuosity squared divided by the porosity (see section 1.3.3.2), it is apparent that with decreasing porosity, tortuosity is also increasing exponentially. So, a greater exponent value for a given sediment results in the tortuosity of that sediment increasing faster as porosity decreases. Between different lithologies, different exponent values are likely caused by different pore structures due to a combination of sediment properties, such as grain shape, size distribution, surface charge, cementation, and organic matter content. However, separate sites with similar lithologies may have a wide range of values of (n), implying that the properties of the constituents of the sediment are not wholly responsible for the pore structure of the sediment.

When the sites are separated by depositional environment as well as lithology, the data show that similar lithologies from different depositional environments have differing ranges of formation factor values for a given porosity range, which is reflected in the different values of the exponent in Archie's formula as listed in Tables 2.6 and 2.7.

Table 2.6. Comparison of Archie's formula exponent values from shallow versus deep depth intervals, with uncertainties. From sites with porosities less than 0.70. ND: Not Determined, for values that could not be determined from the ODP data.

Sediment Type	Depositional Environment	10 mbsf		50 mbsf	
		n-value	scatter	n-value	scatter
Calcareous Ooze	Slope	2.5	0.5	2.25	0.5
	Margin Plateau	2	0.5	2	0.5
	Ridge	ND	ND	1.5	0.75
Mud	Slope	2.5	0.5	ND	ND
	Basin	2	0.75	3	ND
Mud + Calcareous Ooze	Slope	2.75	0.5	2.75	0.5
	Ridge	ND	ND	1.25	ND
Mud + Sand	Slope	2	0.5	2.25	0.5
	Basin	1	ND	2	0.5

Table 2.7. Comparison of Archie's formula exponent values from shallow versus deep depth intervals, with uncertainties. From sites with porosities greater than 0.70. ND: Not Determined, for values that could not be determined from the ODP data.

Sediment Type	Depositional Environment	10 mbsf		50 mbsf	
		n-value	scatter	n-value	scatter
Siliceous Ooze	Slope	3.5	ND	ND	ND
Mud	Basin	3.5	0.75	3.75	1
Mud + Calcareous Ooze	Slope	3.5	ND	3.5	0.5
Mud + Siliceous Ooze	Slope	ND	ND	3	ND
	Basin	4.5	ND	3.25	1
	Ridge	3.5	0.75	3.5	ND
Calcareous + Siliceous Ooze	Basin	3.25	ND	3	0.5

This suggests depositional environment has some control over the pore structure of sediment, independent of sediment type. The type of deposition could

possibly give the sediment grains a tendency to be oriented and sorted differently from lithologically similar sediment deposited by a different process, creating different pore structures. Also, physical and biological processes acting on the sediment after deposition could influence grain orientation, and thus pore structure, such as wave action on continental shelves or bioturbation in the top few meters of sediment.

Assuming similar depositional environments have similar types of deposition and similar processes at work on the sediment after deposition, sediments of similar lithologies from similar depositional environments should have similar exponents in the Archie formula. Thus, separating the data into the four depositional environments of continental margin slope, continental margin plateau, deep ocean basin, and deep ocean ridge, the values of the exponent (n) in Archie's formula, for the various lithologies, can be estimated with greater precision than by categorizing sediments by lithology alone.

The ODP data with similar lithologies from different depositional environments do have different values of the exponent in Archie's formula, as listed in Tables 2.6 and 2.7. The differences between most are not outside of the uncertainty, but they do occupy different ranges. The value of the exponent (n) in Archie's formula (Archie, 1942) can be estimated with an uncertainty of about +/- 0.5 for continental margin sites which are separated by both lithology and depositional environment between porosities of 0.50 and 0.85. The value of the exponent can be determined with an uncertainty ranging from +/- 0.5 to +/- 1.0 for basin and ridge sites. If these sites were not separated by depositional environment, the uncertainty would be greater for

all lithologies. This suggests that, without knowing the specifics of each site's depositional history, the general depositional environment may be used to constrain the relationship between porosity and tortuosity further than with lithology alone.

Most of the lithologies listed with porosities above 0.70 have no data for porosities lower than 0.70. However, the available data for the mud and the mud + calcareous ooze lithologies exhibit an increase in the value of the exponent of Archie's formula of 0.5-1.5 at porosities greater than 0.70, which is similar to the 0.5-1.0 increase observed by Ullman and Aller, (1982). While this increase in the value of the exponent is reported with no discussion of possible causes in Ullman and Aller, (1982), it seems reasonable to assume that different pore structures dominate the tortuosity of fine-grained sediment at porosities above 0.70 than below 0.70. Perhaps some sediments lose secondary pore structures or grain-to-grain contact occurs at 70% porosity and lower. The effect organic matter may have on the relationship between porosity and formation factor over all porosity ranges is also not known. No data are reported for sediments other than mud or mud mixed with calcareous oozes which span the 0.70 porosity value, so there is no evidence of whether this jump in exponent value exists for other lithologies.

2.5.3 Consistency between Depth Intervals

In order to determine that average values of porosity may be used to estimate the value of the formation factor using Archie's formula, it must be demonstrated that the values of the adjustable constants are not significantly dependant on the depth being averaged, down to 50 meters below the seafloor (mbsf). Value ranges of the

Archie exponent are determined for each lithology/depositional environment category for depth intervals of 0-10 mbsf and 0-50 mbsf from Figures 2.8-2.11. Ranges of exponent values were determined to the nearest 0.25 from the plots. It should be noted that all 10 meter depth interval lithology/depositional environment categories cannot be used for the 50 meter plots and vice-versa, due to data availability. See section 2.3.3 for details on minimum data qualifications for the two depth intervals. The exponent ranges are compared and not found to be significantly different between these two depth intervals (Tables 2.6 and 2.7). Between sediments for which Archie exponent uncertainty is determined (Slope and plateau calcareous ooze, slope mud + calcareous ooze, slope mud + sand, basin mud over 0.70 porosity), the maximum difference between (n) values was 0.25 with uncertainties of 0.5. There are three lithologies which have greater differences (basin mud, basin mud + sand, basin mud + siliceous ooze over 0.70 porosity), however the uncertainty of at least one exponent value, either above or below 0.70 porosity, for each are not able to be determined with existing data, so cannot be evaluated.

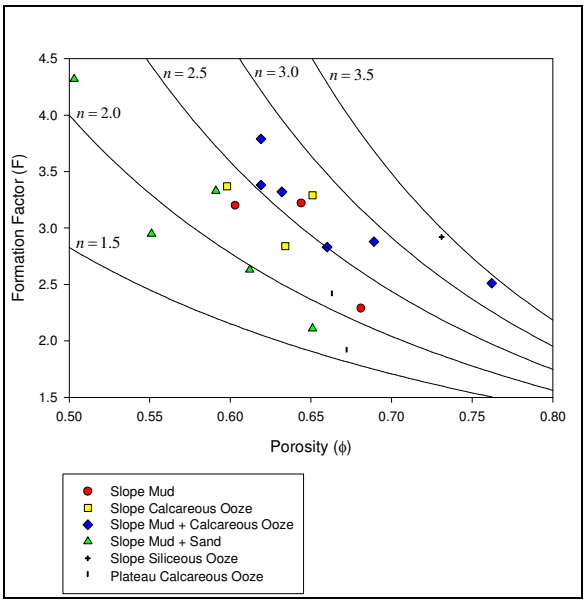

Figure 2.8. Plot of continental margin data from top 10m of sediment, categorized by lithology and depositional environment; plotted with the estimation curves of Archie's formula.

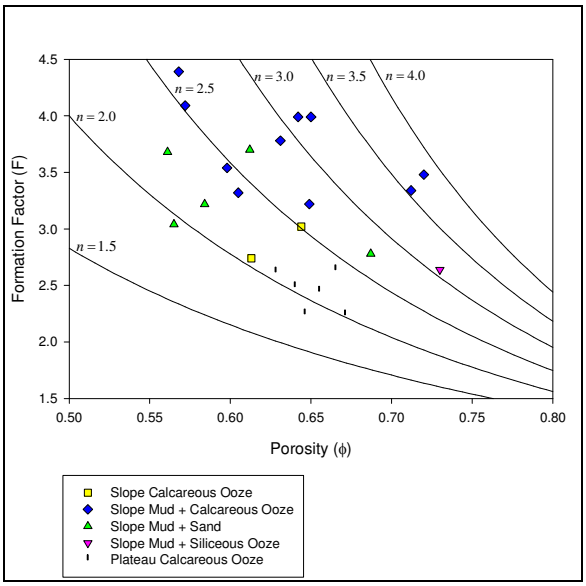

Figure 2.9. Plot of continental margin data from top 50m of sediment, categorized by lithology and depositional environment; plotted with the estimation curves of Archie's formula.

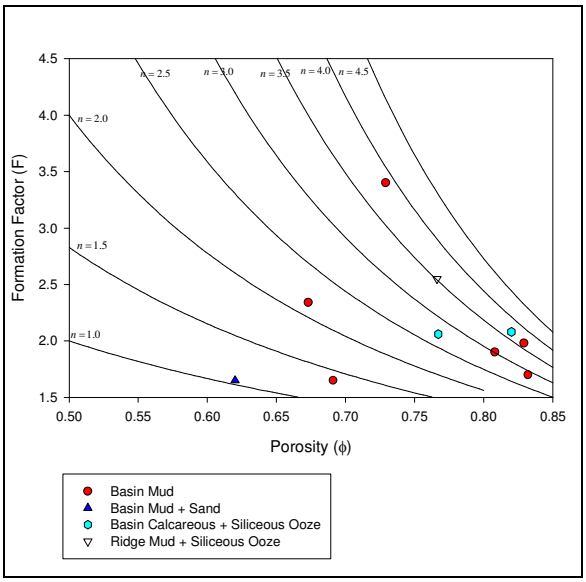

Figure 2.10. Plot of deep ocean basin and ridge data from top 10m of sediment, categorized by lithology and depositional environment; plotted with the estimation curves of Archie's formula.

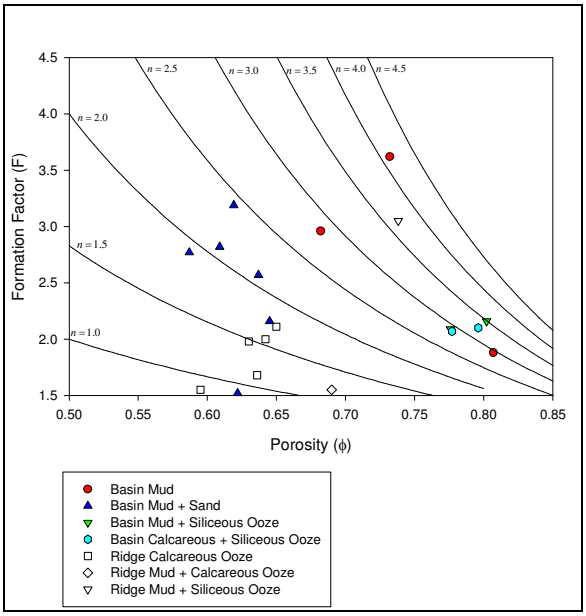

Figure 2.11. Plot of deep ocean basin and ridge data from top 50m of sediment, categorized by lithology and depositional environment; plotted with the estimation curves of Archie's formula.

2.6 Conclusions

By categorizing sediment by both depositional environment and lithology, the relationship between porosity and formation factor can be determined with greater precision than can be achieved by categorizing sediment by lithology alone.

The value of the exponent in Archie's formula does not change significantly from the shallower (~10 mbsf) to the deeper (~50 mbsf) sediments of continental margin sites with similar porosities, depositional environments, and lithologies.

Values of the exponent (n) in Archie's formula can be estimated based on depositional environment, lithology, and porosity (Tables 2.8 and 2.9).

Table 2.8. Exponent with uncertainty for Archie's formula based on sediment lithology and depositional environment with porosity less than 0.70.

Sediment Type	Depositional Environment	Exponent	Uncertainty
Calcareous Ooze	Slope	2.5	0.5
	Margin Plateau	2.0	0.5
	Ridge	1.25	0.5
Mud	Slope	2.5	0.5
	Basin	2.0	1.0
Mud + Calcareous Ooze	Slope	2.75	0.5
	Ridge	1.25	ND
Mud + Sand	Slope	2.25	0.5
	Basin	1.5	1.0

Table 2.9. Exponent with uncertainty for Archie's formula based on sediment lithology and depositional environment with porosity greater than 0.70.

Sediment Type	Depositional Environment	Exponent	Uncertainty
Siliceous Ooze	Slope	3.5	ND
Mud	Basin	3.5	1.0
Mud + Calcareous Ooze	Slope	3.5	0.5
Mud + Siliceous Ooze	Slope	3.0	ND
	Basin	3.25	ND
	Ridge	3.5	ND
Calcareous + Siliceous Ooze	Basin	3.0	ND

The value of the exponent (n) in Archie's formula increases by 0.5-1.5 at porosity values above 0.70 for fine-grained sediments.

2.7 References

Archie, G.E., 1942. The electrical resistivity log as an aid in determining some reservoir characteristics. *Petroleum Transactions American Institute of Mining, Metallurgical, and Petroleum Engineers,* **146**, 54–62.

Atkins, E.R., Jr. and Smith, G.H., 1961. The significance of particle shape in formation resistivity factor-porosity relationships. *Journal of Petroleum Technology*, **13**, 285-291.

Boudreau, B.P., 1996. The diffusive tortuosity of fine-grained unlithified sediments. *Geochimica et Cosmochimica Acta*, **60**, 3139-3142.

Kennett, J.P., 1982. *Marine Geology*. Prentice-Hall, Inc.

Iversen, N. and Jorgensen, B.B., 1993. Diffusion Coefficients of sulfate and methane in marine sediments: Influence of porosity. *Geochimica et Cosmochimica Acta*, **57**, 571-578.

Low, P.F., 1981. Principles of ion diffusion in clays. In *Chemistry in the Soil Environment*; American Society of Agronomy Special Publication, **40**, 31-45.

Ullman, W.J. and Aller, R.C., 1982. Diffusion coefficients in nearshore marine sediments. *Limnology and Oceanography*, **27**, 552-556.

Weissberg, H.L., 1963. Effective Diffusion Coefficient in Porous Media. *Journal of Applied Physics*, **34**, 2636.

APPENDIX A

ODP and IODP Drilling Site Descriptions for Chapter 1

Subduction Zone Sites

ODP Leg 112

One site is used from ODP Leg 112, which drilled into the continental margin off the coast of Peru in the Peru subduction zone. Site 684 is located on the upper slope of the Peru Margin at a water depth of 438 meters.

ODP Leg 170

Three sites are used from ODP Leg 170, which drilled into the continental margin off the western coast of Costa Rica in the Middle-America subduction zone. Site 1040 is located on the lower slope at a water depth of 4177 meters. Site 1041 is located on the lower slope at a water depth of 3306 meters. Site 1043 is located on the lower slope at a water depth of 4313 meters.

ODP Leg 190

Three sites are used from ODP Leg 190, which drilled into the continental margin off the eastern coast of Japan in the Nankai subduction zone. Site 1175 is located on the lower slope at a water depth of 2998 meters. Site 1176 is located on the lower slope at a water depth of 3021 meters. Site 1178 is located on the mid-slope at a water depth of 1742 meters.

ODP Leg 201

One site is used from ODP Leg 201, which drilled into the continental margin off the coast of Peru in the Peru subduction zone. Site 1227 is in close proximity to Site 684 from ODP Leg 112, on the upper slope at a water depth of 427 meters.

ODP Leg 204

Three sites are used from ODP Leg 204, which drilled into Hydrate Ridge, on the Oregon continental margin, in the Cascadia subduction zone. Site 1244 is located on the eastern flank of Hydrate Ridge, at a water depth of 895 meters. Site 1245 is located on the western flank of Hydrate Ridge, at a water depth of 869 meters. Site 1247 is located on the western flank of Hydrate Ridge, at a water depth of 834 meters.

IODP Expedition 311

Three sites are used from IODP Expedition 311, which drilled into the continental margin off the coast of British Columbia, in the Cascadia subduction zone. Site 1326 is located on the flank of an uplifted ridge on the lower slope, at a water depth of 1828 meters. Site 1327 is located on the mid-slope, at a water depth of 1305 meters. Site 1329 is located on the upper slope, at a water depth of 950 meters.

Non-Subduction Margin Sites

ODP Leg 117

Three sites are used from ODP Leg 117, which drilled into the continental margin off the Oman margin in the Indian Ocean. Site 723 is located on the upper

slope at a water depth of 805 meters. Site 724 is located on the upper slope at a water depth of 591 meters. Site 728 is located mid-slope at a water depth of 1422 meters

ODP Leg 150

One site is used from ODP Leg 150, which drilled into the continental margin off the coast of New Jersey in the North-West Atlantic Ocean. Site 906 is located on the upper slope at a water depth of 913 meters.

ODP Leg 155

Three sites are used from ODP Leg 155, which drilled into the Amazon Fan on the continental margin off the coast of Brazil. Site 931 is located on the middle fan at a water depth of 3475 meters. Site 940 is located on the middle fan at a water depth of 3191 meters. Site 944 is located on the middle fan at a water depth of 3701 meters.

ODP Leg 164

Five sites are used from ODP Leg 164, which drilled the Carolina Slope and the Blake Ridge on the continental margin off the coast of the South-Eastern United States. Site 991 is located on the Cape Fear Diapir, mid-slope at a water depth of 2568 meters. Site 993 is located on the Cape Fear Diapir, mid-slope at a water depth of 2642 meters. Site 994 is located on the Blake Ridge at a water depth of 2798 meters. Site 995 is located on the Blake Ridge at a water depth of 2777 meters. Site 997 is located on the Blake Ridge at a water depth of 2770 meters.

ODP Leg 167

Three sites are used from ODP Leg 167, which drilled the California continental margin in the North-East Pacific Ocean, south of the Mendocino triple-

junction. Site 1013 is located in the extensional San Nicolas Basin at a water depth of 1564 meters. Site 1017 is located on the upper slope at a water depth of 955 meters. Site 1022 is located mid-slope at a water depth of 1926 meters.

ODP Leg 172

Five sites are used from ODP Leg 172, which drilled the Carolina Slope and Blake Ridge on the continental margin off the coast of the South-East United States. Site 1054 is located on the upper Carolina Slope at a water depth of 1294 meters. Site 1055 is located on the upper Carolina Slope at a water depth of 1798 meters. Site 1059 is located on the Blake Ridge at a water depth of 2985 meters. Site 1060 is located on the Blake Ridge at a water depth of 4044 meters. Site 1061 is located on the Blake Ridge at a water depth of 4044 meters.

ODP Leg 175

Nine sites are used from ODP Leg 175, which drilled the continental margin off the west coast of Africa. Site 1075 is located on the lower slope at a water depth of 2995 meters. Site 1076 is located on the upper slope at a water depth of 1404 meters. Site 1077 is located on the lower slope at a water depth of 2380 meters. Site 1078 is located on the upper slope at a water depth of 427 meters. Site 1079 is located on the upper slope at a water depth of 738 meters. Site 1082 is located mid-slope at a water depth of 1279 meters. Site 1083 is located on the lower slope at a water depth of 2178 meters. Site 1085 is located mid-slope at a water depth of 1713 meters.

APPENDIX B

DSDP, ODP, and IODP Data Sources

Data from the Ocean Drilling Program (ODP) and Integrated Ocean Drilling Program (IODP) not referenced in the Chapters, such as interstitial water chemistry, porosity, grain density, total organic carbon, site/hole data, etc., were obtained from the Integrated Ocean Drilling Program's online database at:

http://iodp.tamu.edu/janusweb/links/links_all.shtml

The world map of drilling locations (Figure 1.2) was modified from the "Combined IODP, ODP, DSDP Sites" map located at:

http://iodp.tamu.edu/scienceops/maps.html

Qualitative data such as site descriptions, topographic maps, seismic profiles, and other data such as sedimentation rates for Ocean Drilling Program sites were obtained from the Proceedings of the Ocean Drilling Program, Initial Reports, located online at:

http://www-odp.tamu.edu/publications/pubs.htm

Qualitative data such as site descriptions, topographic maps, seismic profiles, and other data such as sedimentation rates for Integrated Ocean Drilling Program sites were obtained from the Integrated Ocean Drilling Program Preliminary Reports, located online at:

http://www.iodp.org/scientific-publications/

Data reviewed from the Deep Sea Drilling Project were located in the Initial Reports of the Deep Sea Drilling Project which can now be found online at:

http://www.deepseadrilling.org/i_reports.htm